ISA Transactions 70 (2017) 357–377

Contents lists available at ScienceDirect

ISA Transactions

journal homepage: www.elsevier.com/locate/isatrans

Explicit analytical tuning rules for digital PID controllers via the magnitude optimum criterion

Konstantinos G. Papadopoulos [a,*], Praveen K. Yadav [b], Nikolaos I. Margaris [a,†]

[a] Aristotle University of Thessaloniki, Department of Electrical & Computer Engineering, GR-54124, Thessaloniki, Greece
[b] Motilal Nehru National Institute of Technology, Department of Electrical Engineering, Allahabad, Uttar Pradesh, India

ARTICLE INFO

Article history:
Received 17 November 2016
Received in revised form
11 June 2017
Accepted 21 June 2017
Available online 5 July 2017

Keywords:
PID control
Optimal sampling time
Digital control
Optimization
Process control
Control engineering
Industrial control

ABSTRACT

Analytical tuning rules for digital PID type–I controllers are presented regardless of the process complexity. This explicit solution allows control engineers 1) to make an accurate examination of the effect of the controller's sampling time to the control loop's performance both in the time and frequency domain 2) to decide when the control has to be I, PI and when the derivative, D, term has to be added or omitted 3) apply this control action to a series of stable benchmark processes regardless of their complexity. The former advantages are considered critical in industry applications, since 1) most of the times the choice of the digital controller's sampling time is based on heuristics and past criteria, 2) there is little a–priori knowledge of the controlled process making the choice of the type of the controller a trial and error exercise 3) model parameters change often depending on the control loop's operating point making in this way, the problem of retuning the controller's parameter a much challenging issue. Basis of the proposed control law is the principle of the PID tuning via the Magnitude Optimum criterion. The final control law involves the controller's sampling time T_s within the explicit solution of the controller's parameters. Finally, the potential of the proposed method is justified by comparing its performance with the conventional PID tuning when controlling the same process. Further investigation regarding the choice of the controller's sampling time T_s is also presented and useful conclusions for control engineers are derived.

1. Introduction

It is by far accepted within the industrial control–automation society that the PID control law offers the simplest and yet most efficient solution to many real–world control problems, [1–8]. In modern control applications, for instance in the field of electrical drives and power electronics [9–12], where controllers are digitally implemented, control engineers still tune the PID parameters based on simple tuning rules, past experience, or heuristics [13,14]. This approach, often leads to poor tuning and unacceptable performance of the control loop in terms of reference tracking and disturbance rejection. Poor tuning is mainly observed in cases where there is little a–priori information regarding the model of the process. A representative example over the industry where poor controller tuning is observed, is the vector control of medium voltage motor drives where the range of switching frequency is often a few hundreds Hz. In this case, the controller's tuning[1] is based often on a simple second order model of the motor and a linear dc gain k_p of the modulation scheme[2]. Since, both motor parameters and the modulator's gain change quite frequently depending on the drive's operating point (change of motor's output frequency), high performance of the drive is not always achieved. Specific parameters in the area of medium voltage drives which are considered to change rather frequently are 1) the affect of the temperature to the rotor time constant [15],[3] 2) variation of the linear dc gain k_p of the pulse width modulator when PWM schemes are followed, [16–19]. In both cases, PI controllers are tuned based on these two parameters. For that reason, many are the cases when poor performance of the drive's control loop is observed, since the aforementioned parameters change frequently while the PI controllers stay tuned with the initial nominal values.

Over the literature, many are the tuning rules that assume the existence of the First Order Lag Plus Dead Time (FOLPDT) model as

* Corresponding author.
† Professor Nikolaos I. Margaris passed away on Monday July 1st, 2013, 1949–2013.
E-mail addresses: konstantinos.papadopoulos@eng.auth.gr (K.G. Papadopoulos), praveen.ee15@mnnit.ac.in (P.K. Yadav).

[1] Speed PI controller and current PI controller in the inner loop.
[2] If pulse width modulation techniques are followed.
[3] Fast variation of rotor resistance due to winding temperature.

http://dx.doi.org/10.1016/j.isatra.2017.06.020
0019-0578/

the basis for developing a control law: a summary of such tuning rules can be found in [20]. These control laws tune the PID's parameters based on the dc gain k_p of the process, the dominant time constant and its time delay d, while ignoring other dynamics of the process. One of these rules which is often used in the area of many industry applications i.e. electrical drives, is the tuning of the PID controller via the well known Magnitude Optimum criterion [21,13]. The principle of the Magnitude Optimum criterion which was introduced by Sartorius and Oldenbourg, is based on the idea of designing a controller which renders the magnitude of the closed loop frequency response as close as possible to unity, in the widest possible frequency range, $|T(j\omega)| \simeq 1$.

In other words, controller parameters are determined such, so that the robustness of the control loop to disturbances occurring at the output of the process, is maximized. Oldenbourg and Sartorius applied the Magnitude Optimum criterion in type–I systems to processes consisting of stable real poles and since then certain works have been proposed towards the method's improvement, [14,22–26].

In this work, the proposed control law extends the application of the Magnitude Optimum criterion to the design of digital PID controllers. Since modern control applications involve digital controller deployment, this work targets on defining an explicit PID solution

1. which tunes the PID controller's parameters explicitly as a function of all modeled process parameters.
2. that involves the sampling time T_s of the controller. Given this explicit solution, control engineers would be able to apply directly the explicit PID tuning conditions and investigate the affect of the sampling time to the control loop's performance both in the time and frequency domain.
3. The analytical expressions regarding the definitions for the P, I and D gains are straightforward and can be easily integrated within the software of a digitally implemented PID controller.

For clearly and properly presenting the proposed method, in Section 2, the explicit solution presented in [27] is shortly presented in Section 2.1, which serves as a fundamental input to the reader to understand the introduction of the sampling time T_s in the proposed control law. Within the same section, the digital implementation of the PID controller is introduced, the analytical proof of which, is presented in Appendix B. In Sections 3, Sections 4 evaluation results are presented focusing on the detrimental effect the choice of the sampling time can have, when regulating the same process via the analog and digital PID controller respectively. The comparison focuses on the control of benchmark process models which are often met over many industry applications. Finally, goal of this work is to provide both the academic and industry society with a feasible control action which shall be able to deliver reliable results that control engineers can reproduce in–house, before deploying the final control action on a real world prototype application.

2. The proposed PID control law

In this section the conventional, revised and the proposed digital PID control action via the Magnitude Optimum criterion is presented. For the paper's consistency, the conventional and the revised analog control law are briefly presented here, since their complete proof has been thoroughly discussed in [14]. The proof of the proposed digital PID control follows the same line as in [14]. In that a general transfer function of the process model is considered and the explicit solution of the gains is derived based on the plant's parameters and the sampling time T_s. The PID control law is presented in Section 2.2, however the whole proof is analytically presented in Appendix B.

2.1. Analog PID controller design

In this section, a short presentation of the analytic tuning rules for analog PID–type controllers via the Magnitude Optimum criterion is presented. Its detailed proof has been presented in [14] and serves as a fundamental input to the reader to further go through the proposed PID digital control law.

To this end, let the plant transfer function consists of $(n-1)$–poles, m–zeros plus a dead time unit in series. Zeros of the plant may lie both in the left or right imaginary half plane. In that, the plant transfer function is defined by

$$G(s) = \frac{s^m\beta_m + s^{m-1}\beta_{m-1} + \cdots + s^2\beta_2 + s\beta_1 + 1}{s^{n-1}\alpha_{n-1} + \cdots + s^3\alpha_3 + s^2\alpha_2 + s\alpha_1 + 1}e^{-sT_d} \quad (1)$$

where $n-1 > m$. The proposed PID–type controller is given by the flexible form

$$C(s) = \frac{1 + sX + s^2Y}{sT_i(1 + sT_{p_n})} \quad (2)$$

allowing its zeros to become conjugate complex. T_{p_n} stands for the unmodelled controller dynamics coming from the controller's implementation. According to Fig. 1, the closed loop transfer function $T(s)$ is given by

$$T(s) = \frac{k_pC(s)G_p(s)}{1 + k_hk_pC(s)G_p(s)} = \frac{N(s)}{D(s)} = \frac{N(s)}{D_1(s) + k_hN(s)}. \quad (3)$$

Polynomials $N(s)$, $D_1(s)$ are equal to

$$N(s) = k_p(1 + sX + s^2Y)\sum_{i=0}^{m}\left(s^i\beta_i\right), \quad (4)$$

$$D_1(s) = sT_ie^{sT_d}\sum_{j=0}^{n}(s^j\alpha_j) \quad (5)$$

respectively, where $\alpha_0 = \beta_0 = 1$ according to (1). Normalizing $N(s)$, $D_1(s)$ by making the substitution $s' = sc_1$ results in

$$N(s') = k_p(1 + s'x + s'^2y)\sum_{i=0}^{m}(s'^iz_i) \quad (6)$$

$$D_1(s') = s't_ie^{s'd}\sum_{j=0}^{n}\left(s'^jr_j\right) \quad (7)$$

respectively. The corresponding normalized terms involved in the control loop are given by $x = \frac{X}{c_1}$, $y = \frac{Y}{c_1^2}$, $t_i = \frac{T_i}{c_1}$, $d = \frac{T_d}{c_1}$, $r_i = \frac{\alpha_i}{c_1^i}$, $\forall\ i = 1, 2, \ldots n,$, $z_j = \frac{\beta_j}{c_1^j}$, $\forall\ j = 1, 2, \ldots m$. The normalized time

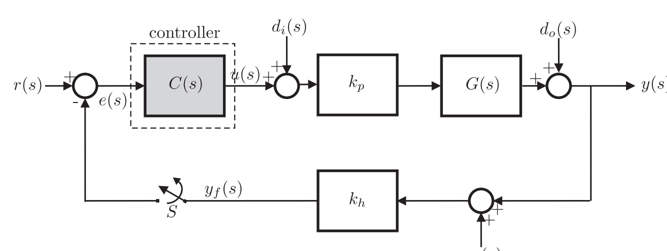

Fig. 1. Block diagram of the closed–loop control system. $G(s)$ is the plant transfer function, $C(s)$ is the controller transfer function, $r(s)$ is the reference signal, $y(s)$ is the output of the control loop, $y_f(s)$ is the output signal after k_h, $d_o(s)$ and $d_i(s)$ are the output and input disturbance signals respectively and $n_o(s)$ is the noise signal process output respectively. k_p stands for the plant's dc gain and k_h is the feedback path. Switch S stands for the border of the open loop transfer function $F_{ol}(s)$ from $r(s)$ to $y_f(s)$.

delay constant d is approximated by the Taylor series

$$e^{s'd} = \sum_{k=0}^{n} \frac{1}{k!} s'^k d^k = 1 + s'^d + \frac{1}{2!} s'^{2d^2} + \frac{1}{3!} s'^{3d^3} + \frac{1}{4!} s'^{4d^4} + \frac{1}{5!} s'^{5d^5} + \cdots. \tag{8}$$

By substituting (8) into (7), $D_1(s')$ becomes

$$D_1(s') = \sum_{i=1}^{k} (t_i s'^i q_{(i-1)}), \quad q_0 = 1, \tag{9}$$

where

$$q_k = \sum_{i=0}^{k} r_{(k-i)} (\frac{1}{i!} d^i), \quad k = 0, 1, 2, \ldots n, \quad r_0 = 1. \tag{10}$$

Polynomials $N(s')$, $D(s') = N(s') + k_h D_1(s')$ are then finally defined by

$$N(s') = \sum_{i=0}^{n} \left[s'^i k_p \left(z_{(i)} + z_{(i-1)} x + z_{(i-2)} y \right) \right], \tag{11}$$

$$D(s') = \sum_{j=0}^{k} s'^j \left[t_i q_{(j-1)} + k_p k_h \left(z_{(j)} + z_{(j-1)} x + z_{(j-2)} y \right) \right] \tag{12}$$

where $z_{(-2)} = z_{(-1)} = 0$, $z_0 = 1$ and $q_{(-1)} = 0$. Therefore, the resulting closed loop transfer function is given by (13).

$$T(s') = \frac{N(s')}{D(s')} = \frac{\sum_{i=0}^{n} \left[s'^i k_p (z_{(i)} + z_{(i-1)} x + z_{(i-2)} y) \right]}{\sum_{j=0}^{k} s'^j \left[t_i q_{(j-1)} + (k_p k_h (z_{(j)} + z_{(j-1)} x + z_{(j-2)} y)) \right]} \tag{13}$$

For proving the revised analog PID control law the optimization conditions of the closed loop transfer function defined in (A.7)–(A.10)[4] are utilized. By sticking to a PID type controller, only four optimization conditions are necessary, see [14].

Optimization condition: $a_0 = b_0$.

From the application of (A.7) to (13) it is obtained

$$k_h = 1. \tag{14}$$

Condition (14) renders the zero order terms of the numerator and denominator polynomial of the closed loop transfer function equal, which means that the closed loop system has zero steady state position error (type–I control loops), see [14,22]. Note that if $k_h = 1$ then $N(s') = \cdots + k_p$ and $D(s') = \cdots + k_p k_h$.

Optimization condition: $a_1^2 - 2a_2 a_0 = b_1^2 - 2b_2 b_0$.

The application of (A.8) to (13) results in

$$t_i = 2k_p k_h (q_1 - z_1 - x) = 2k_p k_h (\sum_{i=0}^{1} (r_{(1-i)} \frac{1}{i!} d^i) - z_1 - x) \tag{15}$$

$$t_i = 2k_p k_h (r_1 + d - z_1 - x) = 2k_p k_h (\frac{\alpha_1}{c_1} + \frac{T_d}{c_1} - \frac{b_1}{c_1} - \frac{X}{c_1}) \tag{16}$$

or $c_1 t_i = 2k_p k_h (\alpha_1 + T_d - b_1 - X)$. If the process consists of stable real poles (T_{p_i}) then $\alpha_1 = \sum_{i=1}^{n} T_{p_i}$. Accordingly, the sum of the plant's zeros (T_{z_i}) is given by $b_1 = \sum_{i=1}^{m} T_{z_i}$. Finally the integral gain is defined by

$$c_1 t_i = 2k_p k_h (\sum_{i=1}^{n} T_{p_i} + T_d - \sum_{i=1}^{m} T_{z_i} - X), \tag{17}$$

or

$$T_i = 2k_p k_h (\sum_{i=1}^{n} T_{p_i} + T_d - \sum_{i=1}^{m} T_{z_i} - X). \tag{18}$$

It is critical to point out the definition of the integral gain contains all the dynamics involved in the closed loop.

Optimization condition: $a_2^2 - 2a_3 a_1 + 2a_4 a_0 = b_2^2 - 2b_3 b_1 + 2b_4 b_0$.

The application of (A.9) to (13) results after some calculus in

$$x - a_{12} y = b_{11} \tag{19}$$

where

$$a_{12} = \frac{q_1 - z_1}{(q_1 - z_1) q_1 - (q_2 - z_2)}, \tag{20}$$

$$b_{11} = \frac{(q_1^2 - 2q_2)(q_1 - z_1) + q_1 z_2 - q_2 z_1 + q_3 - z_3}{(q_1 - z_1) q_1 - (q_2 - z_2)}. \tag{21}$$

Note that a_{12}, b_1 depend explicitly on process parameters.

Optimization condition: $a_3^2 + 2a_1 a_5 - 2a_6 a_0 - 2a_4 a_2 = b_3^2 + 2b_1 b_5 - 2b_6 b_0 - 2b_4 b_2$.

In similar fashion, the application of (A.9) to (13) results in

$$x + a_{22} y = b_{22} \tag{22}$$

where

$$a_{22} = \frac{q_1 z_2 - q_2 z_1 + q_3 - z_3}{q_2^2 - 2q_1 q_3 - q_2 z_2 + q_1 z_3 + q_3 z_1 + q_4 - z_4} \tag{23}$$

and

$$b_{22} = \frac{Q_0 Q_1 + Q_2}{Q_3} \tag{24}$$

where

$$Q_0 = q_2^2 - 2q_1 q_3 + 2q_4 \tag{25}$$

$$Q_1 = q_1 - z_1 \tag{26}$$

$$Q_2 = q_2 z_3 - q_3 z_2 - q_1 z_4 + q_4 z_1 - q_5 + z_5 \tag{27}$$

$$Q_3 = q_2^2 - 2q_1 q_3 - q_2 z_2 + q_1 z_3 + q_3 z_1 + q_4 - z_4. \tag{28}$$

In compact form, the final optimal control law is defined by

$$\begin{bmatrix} 1 & 2k_p k_h & 0 \\ 0 & 1 & -a_{12} \\ 0 & 1 & a_{22} \end{bmatrix} \begin{bmatrix} t_i \\ x \\ y \end{bmatrix} = \begin{bmatrix} 2k_p k_h (q_1 - z_1) \\ b_1 \\ b_2 \end{bmatrix} \tag{29}$$

or finally by

$$\begin{bmatrix} t_i \\ x \\ y \end{bmatrix} = \begin{bmatrix} 1 & 2k_p k_h & 0 \\ 0 & 1 & -a_{12} \\ 0 & 1 & a_{22} \end{bmatrix}^{-1} \begin{bmatrix} 2k_p k_h (q_1 - z_1) \\ b_1 \\ b_2 \end{bmatrix}. \tag{30}$$

From the definition of the integrator's gain

[4] A straightforward approach of the Magnitude Optimum criterion is being presented in the Appendix. The optimization conditions serve for determining the proposed optimal control law.

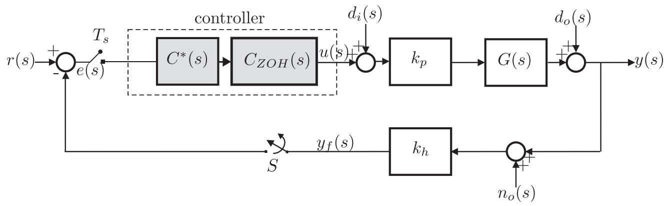

Fig. 2. Block diagram of the closed–loop control system with the digital controller. $G(s)$ is the plant transfer function, $C(s)$ is the controller transfer function, $C_{ZOH}(s)$ the transfer function of the zero order hold unit, sampling T_s is equal to the ZOH sampling time, $r(s)$ is the reference signal, $y(s)$ is the output of the control loop, $y_f(s)$ is the output signal after k_h, $d_o(s)$ and $d_i(s)$ are the output and input disturbance signals respectively and $n_o(s)$ is the noise signals at process output. k_p stands for the plant's dc gain and k_h is the feedback path.

$$T_i = 2k_pk_h\left(\sum_{i=1}^{n}(T_{p_i}) + T_d - \sum_{i=1}^{m}(T_{z_i}) - X\right). \tag{31}$$

it is apparent that $T_i < 0$ if $\left(\sum_{i=1}^{n}(T_{p_i}) + T_d < \sum_{i=1}^{m}(T_{z_i}) + X\right)$.

In that, for the existence of a feasible control the sum of time constants $\sum_{i=1}^{n}(T_{p_i})$ standing for the poles of the process plus the time delay T_d must always be greater than the sum of time constants of zeros of the open loop transfer function. Note that $X = T_n + T_v$, so by applying PID control action to a process with large zeros, PI control can still be retained so that $T_i > 0$ becomes positive again. In this case the derivative term is redundant and has to be omitted.

If PID control is to be retained, the controller can be cascaded with a first order low pass filter of time constant T_x in series of the PID controller, so that the integrator's time constant $T_i > 0$, becomes positive again.
In this case, the new integral gain is given by

$$T_i = 2k_pk_h\left(\sum_{i=1}^{n}(T_{p_i}) + T_d + T_x - \sum_{i=1}^{m}(T_{z_i}) - X\right). \tag{32}$$

Finally, the PID–Lag controller is determined by

$$C_{PID-Lag}(s) = \frac{(1 + sX + s^2Y)}{sT_i(1 + sT_{p_n})}\frac{1}{(1 + sT_x)} \tag{33}$$

2.2. Digital PID controller design–the proposed control law

In this section the proposed digital PID control action is presented while its proof takes place in Section Appendix B. In the following analysis the sampling time T_s of the controller is introduced, which finally is involved within the explicit definition of the PID control action.

For proceeding with the proof, let the stable process in Fig. 2 be defined again by (1). The proposed PID type controller is given by

$$C(s) = C^*(s)C_{ZOH}(s) = \left(\frac{1 + sX + s^2Y}{sT_i(1 + sT_{p_n})}\right)^*\left(\frac{1 - e^{-sT_s}}{sT_s}\right) \tag{34}$$

where the $C^*(s)$ controller stands for the digital representation of the analog PID control law. $C_{ZOH}(s)$ stands for the zero order hold unit and T_s stands for the controller sampling period.

Intermediate calculations of the product $C(s)G(s)$ are presented in Appendix B. The analysis proceeds by normalizing all time constants in the frequency domain with the sampling period T_s of the zero order hold. In that, $s' = sT_s$ is set and the resulting expressions (B.2) and (1) take the form

$$G(s') = k_p\frac{s'^m z_m + \cdots + s'^4 z_4 + s'^3 z_3 + s'^2 z_2 + s' z_1 + 1}{s'^n r_n + s'^{n-1} r_{n-1} + \cdots + s'^5 r_5 + s'^4 r_4 + s'^3 r_3 + s'^2 r_2 + s' r_1 + 1}e^{-s'd} \tag{35}$$

and

$$C(s') = C^*(s')C_{ZOH}(s') = \left(\frac{1 + s'x + s'^2y}{s't_i}\right)^*\left(\frac{1 - e^{-s'}}{s'}\right) \tag{36}$$

whereas the problem statement is as follows: given Eqs. (35), (36) define explicitly the tuning formulas for parameters x, y, t_i and the feedback path k_h as a function of plant's parameters k_p, z_j, r_i, d, the sampling time of the controller T_s, or $x = f_1(k_p, z_j, r_i, T_s)$, $y = f_2(k_p, z_j, r_i, T_s)$, $t_i = f_3(k_p, z_j, r_i, T_s)$.

As analytically proved in Section Appendix B the optimal digital PID control action is defined by

$$k_h = 1. \tag{37}$$

$$t_i = 2k_hk_p(r_1 + d - z_1 - x - \frac{1}{2}) \tag{38}$$

$$\hat{x} - a_1\hat{y} = b_1 \quad \text{and} \quad \hat{x} - a_2\hat{y} = b_2 \tag{39}$$

where

$$a_1 = \frac{2(q_2^2 - q_3) - (q_2y_2 - y_3)}{(q_2^2 - q_3) - (q_2x_2 - x_3)} \tag{40}$$

$$b_1 = \frac{(q_3z_1 - q_2z_2 + z_3 - q_4) - (q_2^2 - 2q_3)(q_2 - z_1)}{(q_2^2 - q_3) - (q_2x_2 - x_3)} \tag{41}$$

$$a_2 = \frac{2q_3^2 - 4q_2q_4 + q_2y_4 - q_3y_3 - y_5 + 2q_5 + q_4y_2}{(q_3 - x_3)q_3 - (q_4 - x_4)q_2 - (q_2 - x_2)q_4 + q_5 - x_5} \tag{42}$$

$$b_2 = \frac{-(q_3^2 - 2q_2q_4 + 2q_5)(q_2 - z_1) + (q_2z_4 - q_3z_3 + q_4z_2 - q_5z_1 - z_5 + q_6)}{(q_3 - x_3)q_3 - (q_4 - x_4)q_2 - (q_2 - x_2)q_4 + (q_5 - x_5)} \tag{43}$$

are process dependent parameters as shown in Appendix B, see Eqs. (B.25), (B.26) and (B.30), (B.31).

By solving (B.30), (B.31) parameters $\hat{x}$, $\hat{y}$ are determined by

$$\hat{x} = \frac{a_1b_2 - a_2b_1}{a_1 - a_2}, \quad \hat{y} = \frac{b_2 - b_1}{a_1 - a_2} \tag{44}$$

where as shown in Appendix B, the controller's parameters x, y are finally determined by

$$x = 2\hat{y} - \hat{x} - 2 \quad \text{and} \quad y = \hat{x} - \hat{y} + 1. \tag{45}$$

respectively. From the definition of the integrator's time constant (38) it is critical to point out that

$$\frac{T_i}{T_s} = 2k_hk_p(r_1 + d - z_1 - x - \frac{1}{2}) \tag{46}$$

or according to (B.14), (B.15)

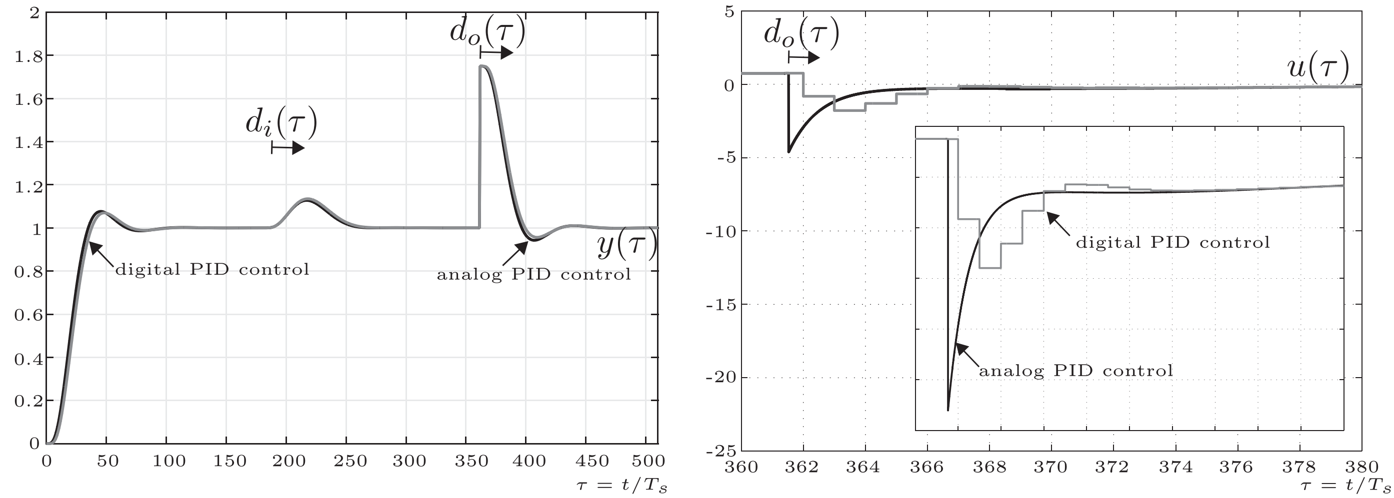

(a) (b)

Fig. 3. Control of a process with dominant time constants. Input disturbance $d_i(s) = 0.25r(s)$ is applied at $\tau = 175$, output disturbance $d_o(s) = 0.75r(s)$ is applied at $\tau = 361$. Sampling time is $\frac{T_{p1}}{T_s} = 10$ (a) Output $y(\tau)$ of the control loop at the presence of input and output disturbances, $\frac{T_{p1}}{T_s} = 10$, $ovs_{an} = 6.9\%$, $ovs_{dig} = 6.6\%$.] (b) Control action $u(\tau)$ at the presence of output disturbance, $\frac{T_{p1}}{T_s} = 10$.

$$\begin{aligned} T_i &= 2k_h k_p(T_s r_1 + T_s d - T_s z_1 - T_s x - \frac{1}{2}T_s) \\ &= 2k_h k_p(p_1 + T_d - \beta_1 - T_s x - \frac{1}{2}T_s) \\ &= 2k_h k_p(\sum_{i=1}^{n}(T_{p_i}) + T_d - \sum_{i=1}^{m}(T_{z_i}) - X - \frac{1}{2}T_s) \end{aligned} \tag{47}$$

In other words and given the definitions of the integrator's time constant in (18) regarding the revised analog PID control law, the integrator's time constant for the proposed PID digital control law is proved to be equal to

$$T_{i_{dig}} = T_{i_{an}} - 2k_h k_p \frac{1}{2}T_s. \tag{48}$$

Note in this case that $T_{i_{dig}}$ and $T_{i_{an}}$ are the optimal values for the integrator's time constant regarding the digital and analog design respectively.

3. Evaluation results

For justifying the potential of the proposed optimal control law a comparison between the analog PID tuning via the Magnitude Optimum criterion, (Section 2.1) and the digital control law (Section 2.2) is carried out. Both closed loop control systems have been normalized with sampling time T_s, $s' = sT_s$. Controller dynamics have been chosen equal to $T_{\Sigma c} = 0.1T_{p_1}$.

For each one of the examples in Sections 3.1–3.3 six figures are presented. Figure (a) focuses on $y(\tau)$ response in the presence of input and output disturbance in the control loop when sampling time is chosen $t_{p_1} = \frac{T_{p1}}{T_s} = 10, 20, 100$.

In Section 3.4 the control of a process with a big zero is investigated. In this example, loss of controllability of the control loop is observed. To overcome this obstacle the proposed PID controller turns into PID–Lag control. In this case, sampling time $\frac{T_{p1}}{T_s} = 40$ remains constant and an investigation of how the lag time constant affects the performance of the control loop is presented.

3.1. A process with dominant time constants

In the first example, the process defined by

$$G(s') = \frac{1}{(1 + 10\,s')(1 + 7.79\,s')(1 + 6.73\,s')(1 + 3.39\,s')(1 + 2.97\,s')} \tag{49}$$

is adopted, for which $\frac{T_{p1}}{T_s} = 10$. Gain k_p has been chosen equal to $k_p = 1$. The analog control action and the corresponding proposed digital control action are given by

$$\begin{aligned} C_{PID-an}(s') &= \frac{1 + s'x + s'^2 y}{s' t_i}\frac{1}{(1 + s' t_{p_n})} \\ &= \frac{1 + 22.42\,s' + 135.1s'^2}{18.91s'^2 + 18.91\,s'} \end{aligned} \tag{50}$$

and

$$C_{PID-dig}(s') = \left(\frac{1 + s'x + s'^2 y}{s' t_i(1 + s' t_{p_n})}\right)^* \frac{(1 - e^{-s'})}{s'} = \frac{1 + 22.96\,s' + 143.6s'^2}{24.32s'^3 + 31.26s'^2 + 20.84s'} \tag{51}$$

respectively. In Fig. 3(a) the step response of both control loops is presented in the presence of input and output disturbance at $\tau = 175$ and $\tau = 361$ with amplitude $d_i(\tau) = 0.25r(\tau)$ and $d_o(\tau) = 0.75r(\tau)$ respectively.

Settling time t_{ss} of $y(\tau)$ in the control loop where the analog controller is incorporated is $t_{ss} = (175 + 61.8)\tau$ and $t_{ss} = (175 + 58.22)\tau$ for the digital control action respectively. Overshoot of the step response is $ovs = 6.9\%$ in case of analog control action and $ovs = 6.6\%$ in case of digital control action.

In Fig. 3(b) the command signal $u(\tau)$ is also presented. In this case, the sampling time T_s has been chosen equal to $t_{p_1} = \frac{T_{p1}}{T_s} = 10$, ten times smaller than the dominant time constant. In Figs. 4(a), (b), 5(a), (b) the sampling time is reduced, and becomes equal to $t_{p_1} = \frac{T_{p1}}{T_s} = 20$ and $t_{p_1} = \frac{T_{p1}}{T_s} = 100$ respectively. This decrease of the sampling time proves to have a detrimental effect in the command signal's amplitude which in many control applications is not acceptable due to constraints on the hardware[5]. Specifically, in Fig. 4

[5] Constraints on the command signal are common in the area of electrical

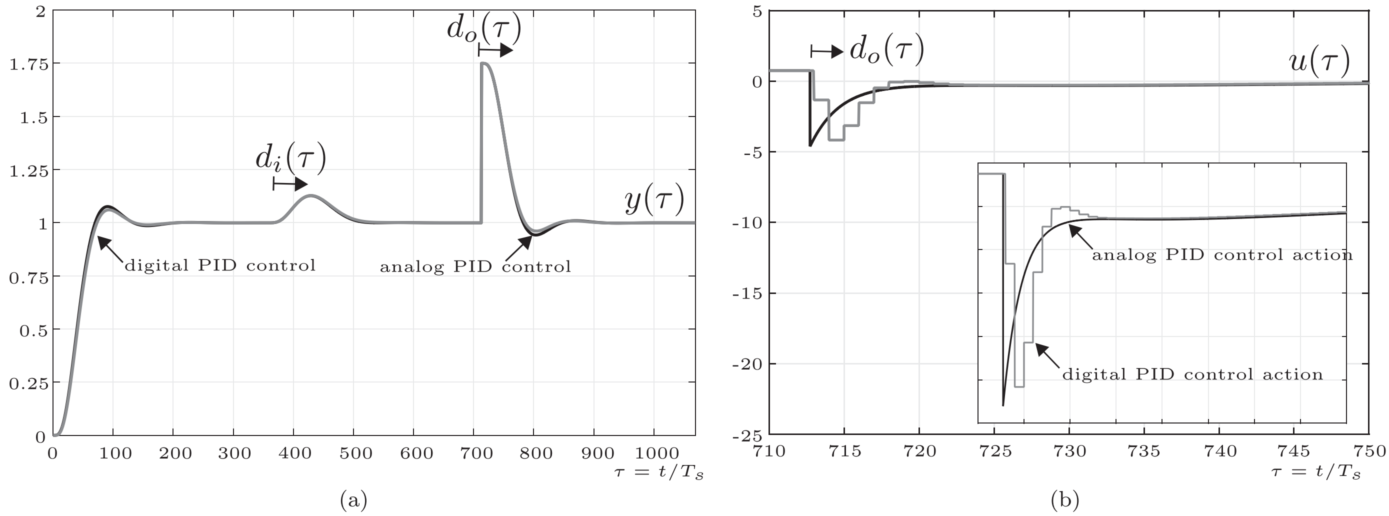

Fig. 4. Control of a process with dominant time constants. Input disturbance $d_i(s) = 0.25r(s)$ is applied at $\tau = 361$, output disturbance $d_o(s) = 0.75r(s)$ is applied at $\tau = 712$. Sampling time is $\frac{T_{p1}}{T_s} = 20$ (a) Output $y(\tau)$ of the control loop at the presence of input and output disturbances, $\frac{T_{p1}}{T_s} = 20$, $ovs_{an} = 7.6\%$, $ovs_{dig} = 6.8\%$. (b) Control action $u(\tau)$ at the presence of output disturbance, $\frac{T_{p1}}{T_s} = 20$.

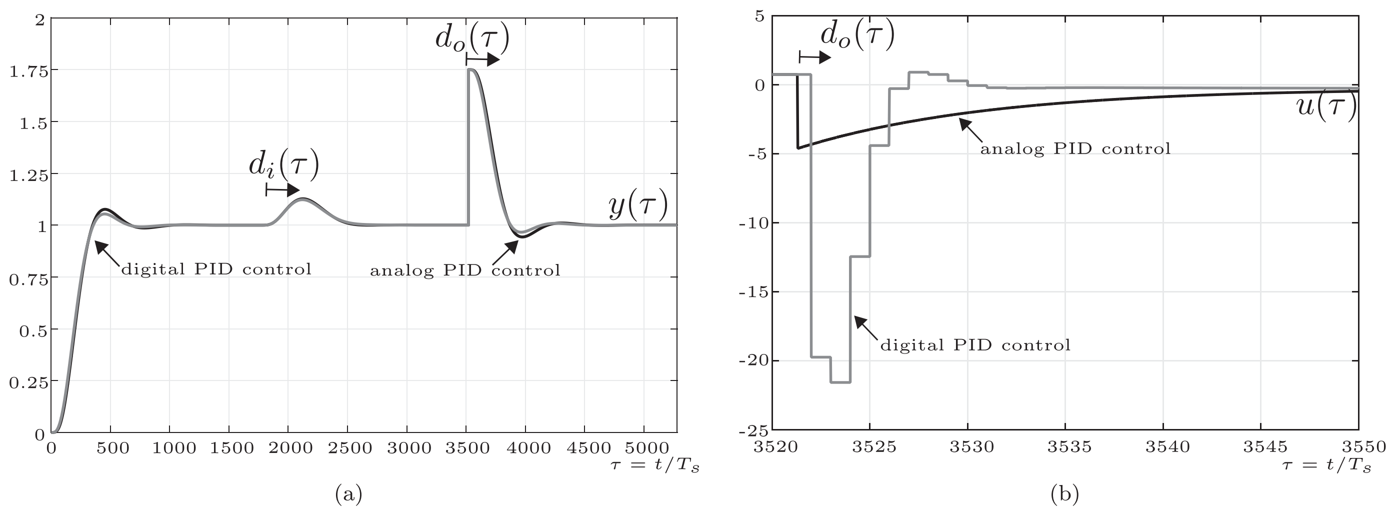

Fig. 5. Control of a process with dominant time constants. Input disturbance $d_i(s) = 0.25r(s)$ is applied at $\tau = 1740$, output disturbance $d_o(s) = 0.75r(s)$ is applied at $\tau = 3521$. Sampling time is $\frac{T_{p1}}{T_s} = 100$ (a) Output $y(\tau)$ of the control loop at the presence of input and output disturbances, $\frac{T_{p1}}{T_s} = 100$, $ovs_{an} = 7.5\%$, $ovs_{dig} = 6.9\%$. (b) Control action $u(\tau)$ at the presence of output disturbance, $\frac{T_{p1}}{T_s} = 100$.

(b) the control effort of the digital controller is comparable with the analog command signal, however in Fig. 5(b) ($t_{p_1} = \frac{T_{p1}}{T_s} = 100$) the peak amplitude of $u(\tau)$ for digital control becomes almost 5 times greater than that of analog control. The calculated controller parameters when $t_{p_1} = \frac{T_{p1}}{T_s} = 20$ and $t_{p_1} = \frac{T_{p1}}{T_s} = 100$ are presented in Sections C.1, C.2 respectively.

3.2. A process with long time delay

In the second example the process defined by

$$G(s') = \frac{1.23e^{-200\,s'}}{(1+100\,s')(1+89\,s')(1+75\,s')(1+66\,s')(1+43\,s')} \quad (52)$$

is considered, for which $\frac{T_{p1}}{T_s} = 10$ has been chosen. The analog control action and the corresponding digital control action are given by

$$C_{PID-an}(s') = \frac{1+s'x+s'^2y}{s't_i}\frac{1}{(1+s't_{p_n})} = \frac{1+26.09\,s'+232.5s'^2}{48.47s'^2+48.47\,s'} \quad (53)$$

and

$$C_{PID-dig}(s') = \left(\frac{1+s'x+s'^2y}{s't_i(1+s't_{p_n})}\right)^* \frac{(1-e^{-s'})}{s'} = \frac{1+29.35\,s'+281.3s'^2}{51.5s'^3+66.21s'^2+44.14s'} \quad (54)$$

respectively. Input $d_i(\tau) = 0.25r(\tau)$ and output $d_o(\tau) = 0.75r(\tau)$ disturbances are applied at 265τ and 530τ respectively. The control loop's response $y(\tau)$ of the analog controller exhibits more attractive characteristics compared to the digital controller both in terms of

(*footnote continued*)
drives introduced by the power electronics circuit. When a voltage–vector is decided to be applied to the machine's terminals, not all combinations are available so that the hardware is protected, see [28].

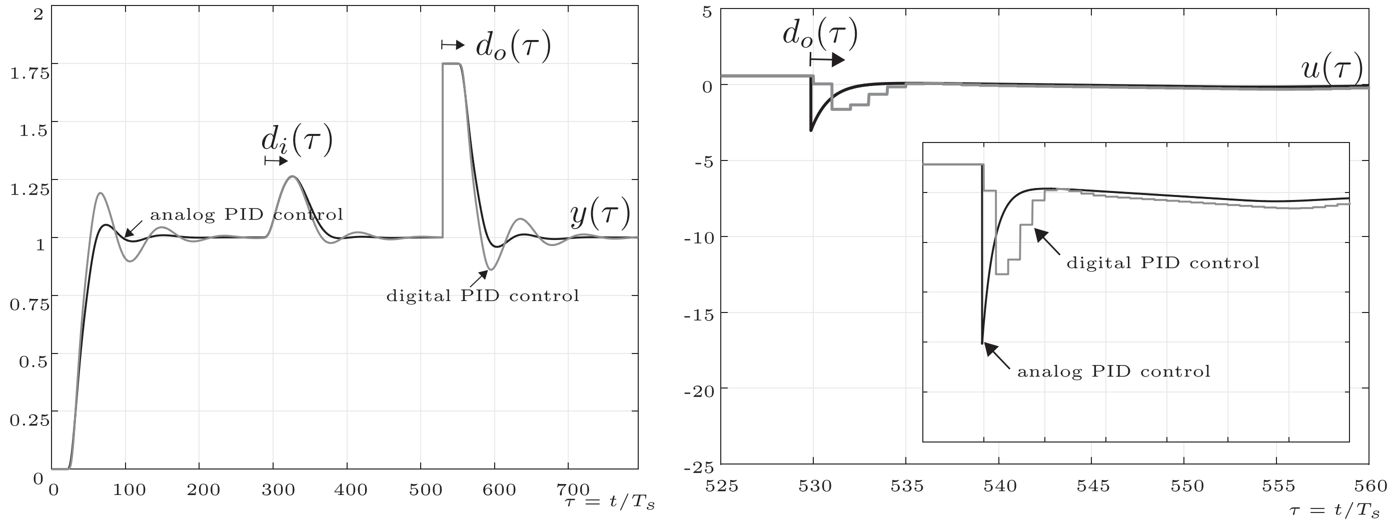

(a) (b)

Fig. 6. Control of a process with long time delay. Input disturbance $d_i(s) = 0.25r(s)$ is applied at $\tau = 265$, output disturbance $d_o(s) = 0.75r(s)$ is applied at $\tau = 530$. Sampling time is $\frac{T_{p_1}}{T_s} = 10$ (a) Output $y(\tau)$ of the control loop at the presence of input and output disturbances, $\frac{T_{p_1}}{T_s} = 10$, $ovs_{an} = 5.3\%$, $ovs_{dig} = 19.2\%$. (b) Control action $u(\tau)$ at the presence of output disturbance, $\frac{T_{p_1}}{T_s} = 10$.

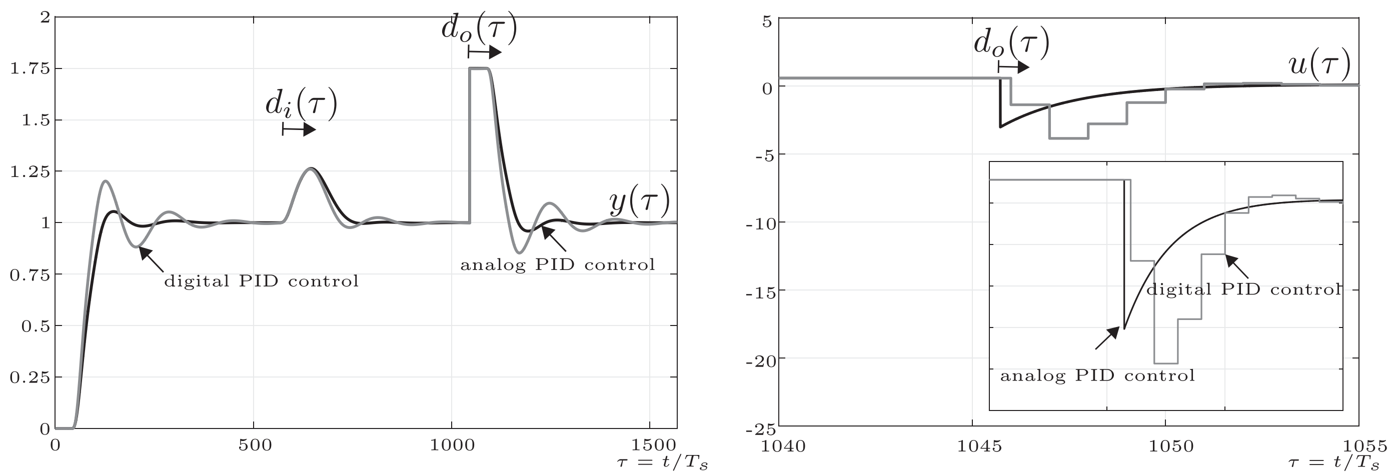

(a) (b)

Fig. 7. Control of a process with long time delay. Input disturbance $d_i(s) = 0.25r(s)$ is applied at $\tau = 565$, output disturbance $d_o(s) = 0.75r(s)$ is applied at $\tau = 1046$. Sampling time is $\frac{T_{p_1}}{T_s} = 20$ (a) Output $y(\tau)$ of the control loop at the presence of input and output disturbances, $\frac{T_{p_1}}{T_s} = 20$, $ovs_{an} = 5.4\%$, $ovs_{dig} = 20.2\%$. (b) Control action $u(\tau)$ at the presence of output disturbance, $\frac{T_{p_1}}{T_s} = 20$.

reference tracking and disturbance rejection, Fig. 6(a). However, as shown in Fig. 6(b), the analog controller spends more effort for achieving this result when $\frac{T_{p_1}}{T_s} = 10$. In case where $t_{p_1} = \frac{T_{p_1}}{T_s} = 20$ the control effort for both controllers becomes almost the same Fig. 7(b). However, when $t_{p_1} = \frac{T_{p_1}}{T_s} = 100$ the command signal's behaviour becomes unacceptable in the digital controller design, see Fig. 8(b) since the peak overshoot becomes almost seven times greater than the initial design $t_{p_1} = \frac{T_{p_1}}{T_s} = 10$. The calculated controller parameters when $t_{p_1} = \frac{T_{p_1}}{T_s} = 20$ and $t_{p_1} = \frac{T_{p_1}}{T_s} = 100$ are presented in Sections C.3, C.4 respectively.

3.3. A non–minimum phase process

In this example the process is described by

$$G(s') = \frac{(1 - 10.9\,s')(1 - 0.45\,s')}{(1 + 20\,s')(1 + 16.2\,s')(1 + 15.91\,s')(1 + 14.5\,s')(1 + 8.39\,s')} \quad (55)$$

consisting of two right half plane zeros. The analog control action and the corresponding digital control action are given by

$$C_{PID-an}(s') = \frac{1 + s'x + s'^2y}{s't_i}\frac{1}{(1 + s't_{p_n})} = \frac{1 + 27.39\,s' + 208.5s'^2}{45.24s'^2 + 45.24\,s'} \quad (56)$$

and

$$C_{PID-dig}(s') = \left(\frac{1 + s'x + s'^2y}{s't_i(1 + s't_{p_n})}\right)^* \frac{(1 - e^{-s'})}{s'} = \frac{1 + 28.02\,s' + 220.6s'^2}{55.5s'^3 + 71.42s'^2 + 47.61s'} \quad (57)$$

respectively. Input $d_i(\tau) = 0.25r(\tau)$ and output $d_o(\tau) = 0.75r(\tau)$ disturbance is applied at 252τ and 505τ respectively, see Fig. 9(a).

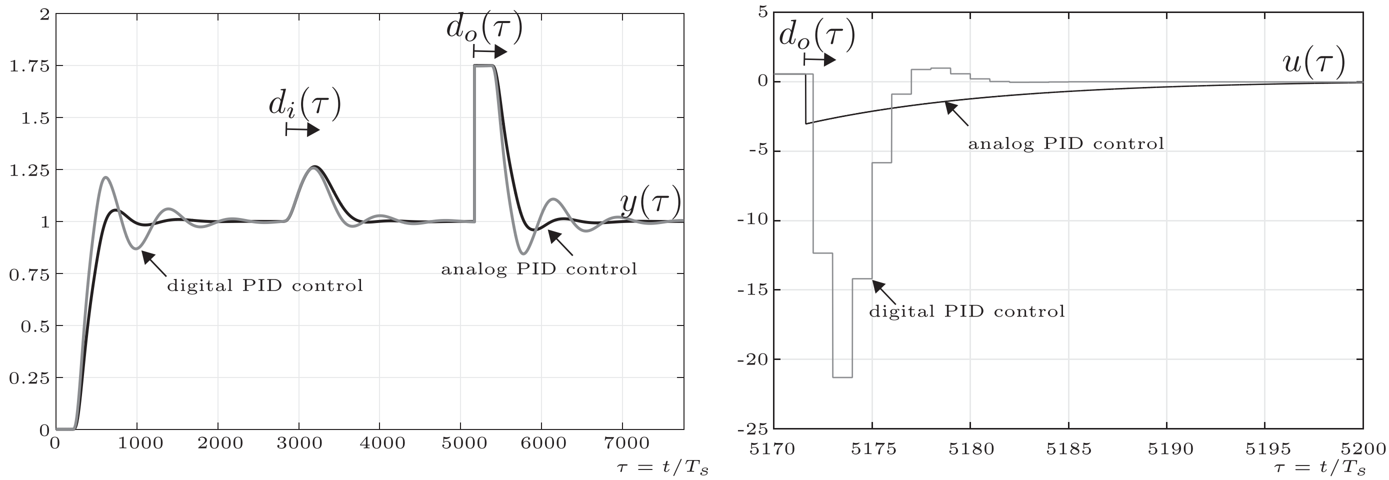

(a) (b)

Fig. 8. Control of a process with long time delay. Input disturbance $d_i(s) = 0.25r(s)$ is applied at $\tau = 2830$, output disturbance $d_o(s) = 0.75r(s)$ is applied at $\tau = 5172$. Sampling time is $\frac{T_{p1}}{T_s} = 100$ (a) Output $y(\tau)$ of the control loop at the presence of input and output disturbances, $\frac{T_{p1}}{T_s} = 100$, $ovs_{an} = 5.4\%$, $ovs_{dig} = 21.1\%$. (b) Control action $u(\tau)$ at the presence of output disturbance, $\frac{T_{p1}}{T_s} = 100$.

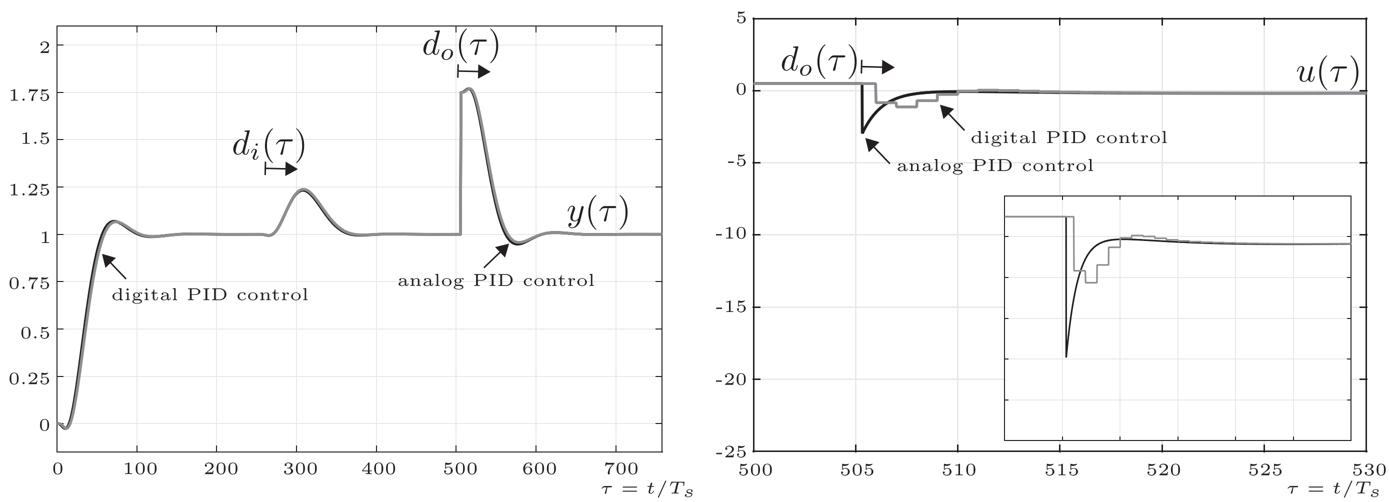

(a) (b)

Fig. 9. Control of a non–minimum phase process. Step response of the closed loop control system. Input disturbance $d_i(s) = 0.25r(s)$ is applied at $\tau = 252$, output disturbance $d_o(s) = 0.75r(s)$ is applied at $\tau = 505$. Sampling time is $\frac{T_{p1}}{T_s} = 10$ (a) Output $y(\tau)$ of the control loop at the presence of input and output disturbances, $\frac{T_{p1}}{T_s} = 10$, $ovs_{an} = 6.9\%$, $ovs_{dig} = 6.5\%$. (b) Control action $u(\tau)$ at the presence of output disturbance, $\frac{T_{p1}}{T_s} = 10$.

From there it is apparent that if $t_{p_1} = \frac{T_{p1}}{T_s} = 10$ then both controller implementations exhibit almost the same behaviour regarding reference tracking, disturbance rejection and command signal response, Fig. 9(a), (b). Rise t_{rt} and settling time t_{ss} for analog and digital design are $t_{rt_{an}} = 28.8\tau$, $t_{rt_{dig}} = 30\tau$ and $t_{ss_{an}} = 93\tau$, $t_{ss_{dig}} = 88.9\tau$ respectively.

If the controller's sampling time T_s is further reduced $t_{p_1} = \frac{T_{p1}}{T_s} = 20$, the command signal effort remains within the same level of the analog controller implementation (Fig. 10(b)). However, if sampling time T_s is chosen such $\frac{T_{p1}}{T_s} = 100$ then the peak value of the digital control effort (Fig. 11(b)) becomes 15 times higher compared to Fig. 9(b). The calculated controller parameters when $t_{p_1} = \frac{T_{p1}}{T_s} = 20$ and $t_{p_1} = \frac{T_{p1}}{T_s} = 100$ are presented in Sections C.5, C.6 respectively.

3.4. A process with a large zero

Let us now consider the process defined by

$$G(s') = \frac{0.0714(1 + 45.6\,s')}{(1 + 40\,s')(1 + 22.4\,s')(1 + 19.6\,s')(1 + 15.6\,s')(1 + 11.2\,s')}. \tag{58}$$

The analog control action and the corresponding digital control action are given by

$$C_{PID-an}(s') = \frac{1 + s'x + s'^2 y}{s't_i}\frac{1}{(1 + s't_{p_n})} = \frac{1 + 56.8\,s' + 1128s'^2}{5.94s'^2 + 1.4854\,s'} \tag{59}$$

and

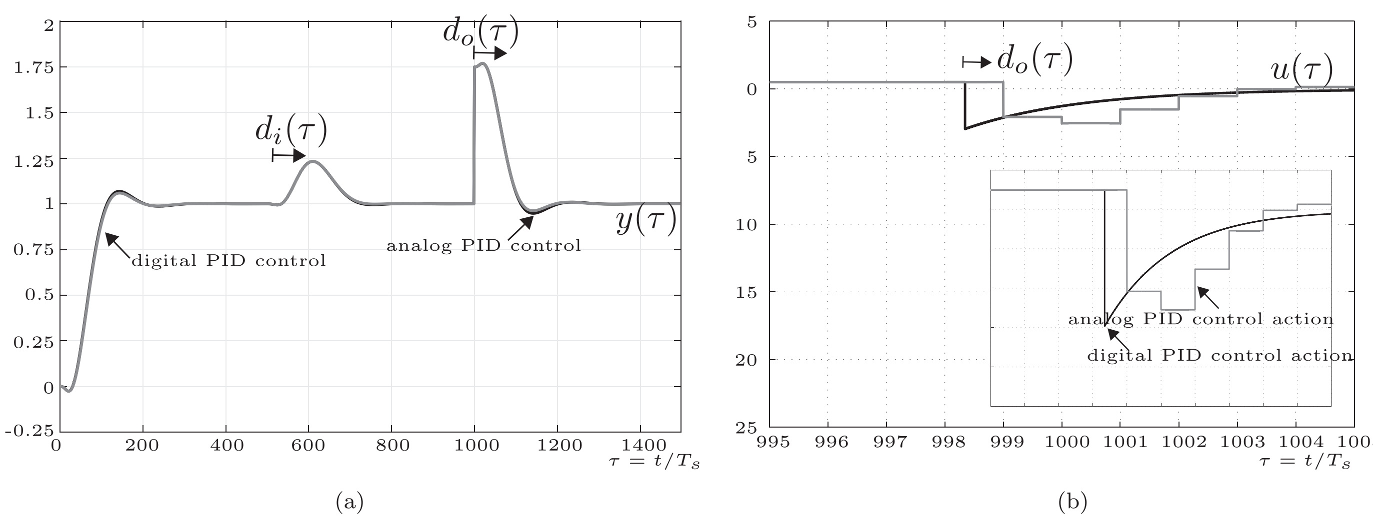

Fig. 10. Control of a non–minimum phase process. Step response of the closed loop control system. Input disturbance $d_i(s) = 0.25r(s)$ is applied at $\tau = 502$, output disturbance $d_o(s) = 0.75r(s)$ is applied at $\tau = 998$. Sampling time is $\frac{T_{p_1}}{T_s} = 20$ (a) Output $y(\tau)$ of the control loop at the presence of input and output disturbances, $\frac{T_{p_1}}{T_s} = 20$, $ovs_{an} = 6.9\%$, $ovs_{dig} = 5.9\%$. (b) Control action $u(\tau)$ at the presence of output disturbance, $\frac{T_{p_1}}{T_s} = 20$.

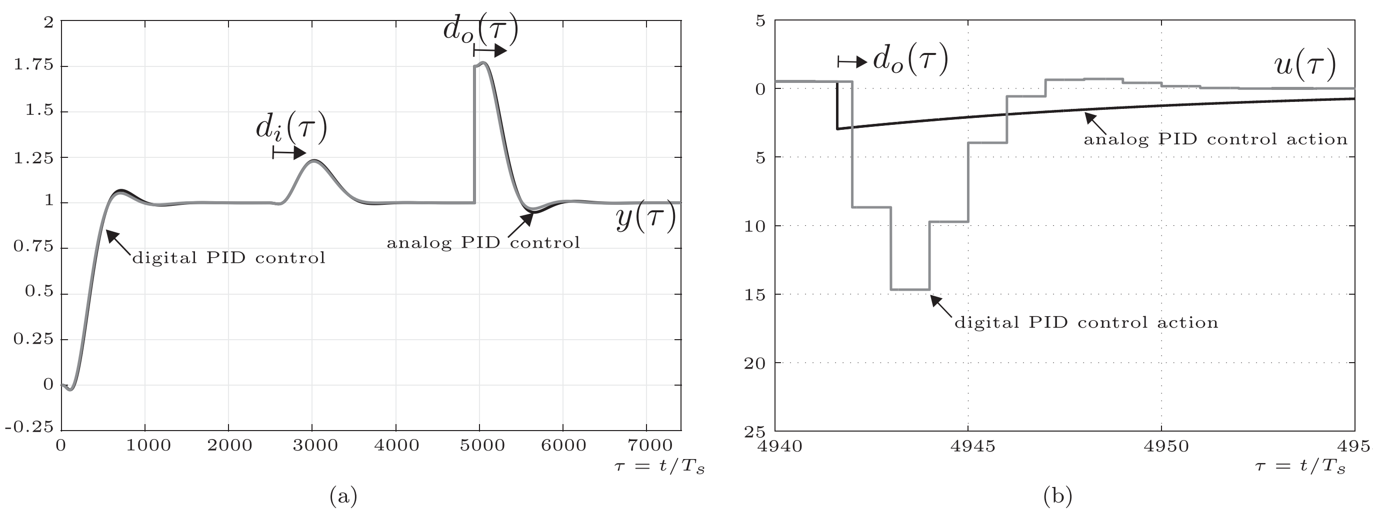

Fig. 11. Control of a non–minimum phase process. Step response of the closed loop control system. Input disturbance $d_i(s) = 0.25r(s)$ is applied at $\tau = 2450$, output disturbance $d_o(s) = 0.75r(s)$ is applied at $\tau = 4942$. Sampling time is $\frac{T_{p_1}}{T_s} = 100$ (a) Output $y(\tau)$ of the control loop at the presence of input and output disturbances, $\frac{T_{p_1}}{T_s} = 100$, $ovs_{an} = 6.9\%$, $ovs_{dig} = 5.4\%$. (b) Control action $u(\tau)$ at the presence of output disturbance, $\frac{T_{p_1}}{T_s} = 100$.

$$C_{PID-dig}(s') = \left(\frac{1 + s'x + s'^2 y}{s' t_i (1 + s' t_{p_n})}\right)^* \frac{(1 - e^{-s'})}{s'}$$
$$= \frac{1 + 60.47\, s' + 1.276 s'^2}{1.372 s'^3 + 1.763 s'^2 + 1.176\, s'} \tag{60}$$

respectively. Controller sampling time has been chosen equal to $\frac{T_{p_1}}{T_s} = 40$. In that case there is a loss of controllability both for the proposed PID type control law, Figs. 12(a), 13(a), since the step response exhibits an overshoot of ovs $\approx$ 35% with unacceptable disturbance rejection. This is due to the fact that the integral gain of the explicit solution gets a very small value $T_{i_{an}} \approx 0$, see (60)[6] resulting in a very fast response leading to an almost uncontrollable closed loop. The aforementioned example result is justified theoretically if we see the explicit solution for the integrator's time constant both for the analog and digital controller implementation.

The revised definition of the integral gain regarding the analog implementation is defined by

$$T_{i_{an}} = 2k_p k_h \left(\sum_{i=1}^{n} T_{p_i} + T_d - \sum_{i=1}^{m} T_{z_i} - X \right), \tag{61}$$

from which it is apparent that $T_{i_{an}}$ becomes negative ($T_{i_{an}} < 0$) when the sum of poles of the open loop transfer function becomes less or equal the sum of zeros of the same function again,

$$\underbrace{\sum_{i=1}^{n} (T_{p_i}) + T_d}_{\text{sum of poles of } F_{OL}} < \underbrace{\sum_{i=1}^{m} (T_{z_i}) + X}_{\text{sum of zeros of } F_{OL}} . \tag{62}$$

According to (48), $T_{i_{dig}} = T_{i_{an}} - 2k_h k_p \frac{1}{2} T_s$ the digital control loop

[6] Integral gain is around unity and will approach the zero value if the sum of zeros in the open loop transfer function becomes equal to the sum of poles of the same function again.

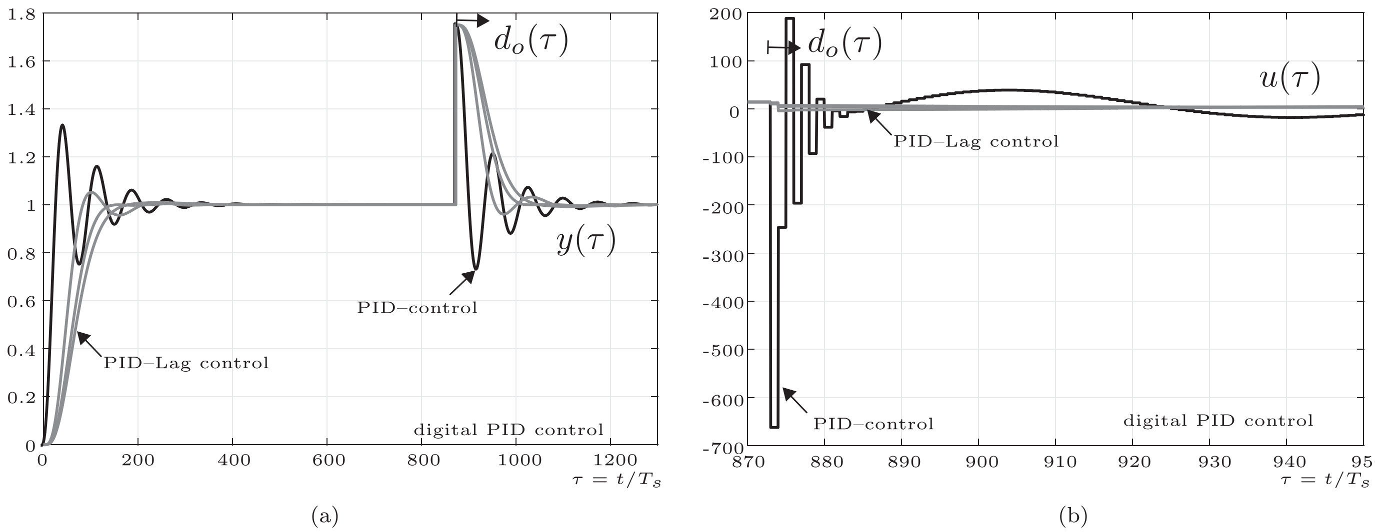

Fig. 12. Control of a process with large zeros. Step response of the closed loop control system. Output disturbance $d_o(s) = 0.75r(s)$ is applied at $\tau = 872$. Sampling time is forty times smaller than the dominant time constant, $\frac{T_{p_1}}{T_s} = 40$ (a) Output $y(\tau)$ of the control loop at the presence of output disturbances, $\frac{T_{p_1}}{T_s} = 40$. (b) Control action $u(\tau)$ at the presence of output disturbance, $\frac{T_{p_1}}{T_s} = 40$.

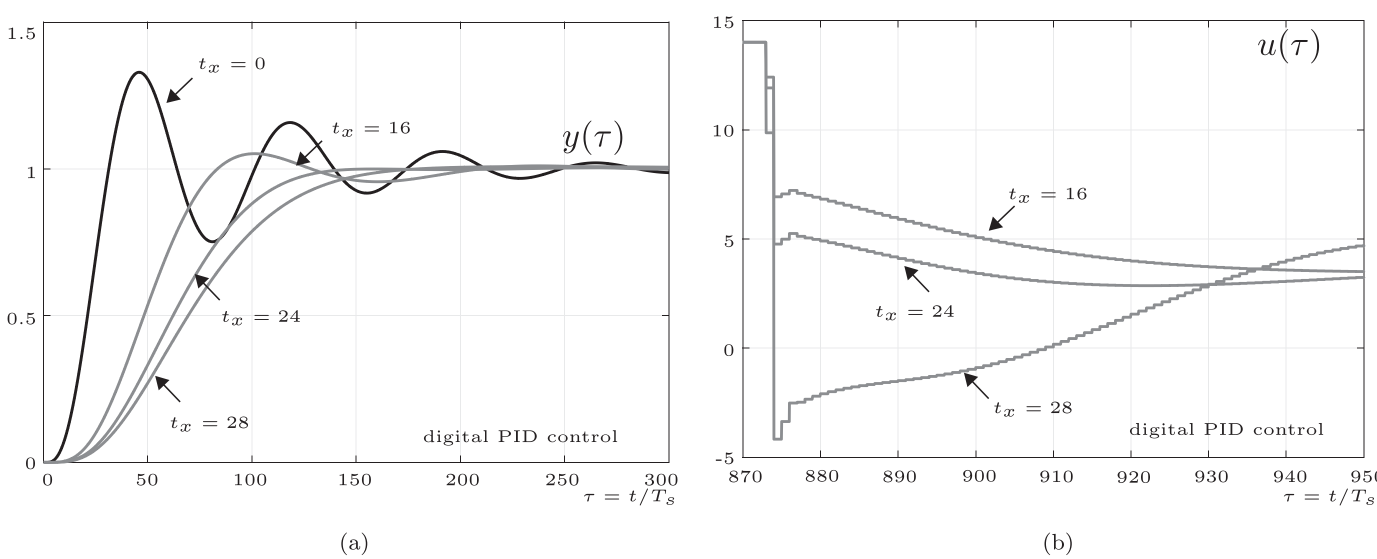

Fig. 13. PID controller turns into PID–Lag control to stabilize the control loop. Choosing a slow time constant t_x=16 stabilizes the control loop. Step response performance metrics, i.e.rise time t_{rt}, settling time t_{ss} can be improved by gradually reducing t_x and making the control loop faster (a) Step response $y(\tau)$ for various values of the t_x lag time constant, $\frac{T_{p_1}}{T_s} = 40$, $ovs_{dig_{t_x=0}} = 33\%$, $ovs_{dig_{t_x=16}} = 5.2\%$, $ovs_{dig_{t_x=24}} = 0\%$, $ovs_{dig_{t_x=28}} = 0\%$. (b) Command signal response $u(\tau)$ for various values of the t_x lag time constant, $\frac{T_{p_1}}{T_s} = 40$.

becomes uncontrollable again for the same aforementioned reason. To that end, $T_{i_{dig}}$ becomes negative ($T_{i_{dig}} < 0$) when

$$\underbrace{\sum_{i=1}^{n}(T_{p_i}) + T_d}_{\text{sum of poles of } F_{OL}} < \underbrace{\sum_{i=1}^{m}(T_{z_i}) + X}_{\text{sum of zeros of } F_{OL}} + \frac{1}{2}T_s. \tag{63}$$

Therefore, for regulating such a process, the control law has to force the sum of poles of the open loop transfer function $F_{OL}(s)$ to become greater than the sum of zeros of $F_{OL}(s)$. To achieve this, the PID controller is turned into PID–Lag control, see (64). The tuning of the lag time constant T_x is presented in the following section. Of course the price paid in this case is that the control loop becomes slower, but finally controllable.

3.4.1. *Tuning of lag time constant T_x*

To overcome the loss of controllability in both cases when $T_{i_{an}} \to 0$ and $T_{i_{dig}} \to 0$, the PID controller proposed in (2), (34) can be turned into PID–Lag controller of the form

$$C_{an}(s) = \frac{1 + sX + s^2Y}{sT_{i_{an}}(1 + sT_{p_n})}\frac{1}{(1 + sT_x)}, \tag{64}$$

$$C_{dig}(s) = \left(\frac{1 + sX + s^2Y}{sT_{i_{dig}}(1 + sT_{p_n})}\right)^{*}\left(\frac{1 - e^{-sT_s}}{sT_s}\right)\frac{1}{(1 + sT_x)}. \tag{65}$$

respectively by adding a first order filter with time constant T_x. In this case the new integrator's time constant for both analog and digital implementation are given by

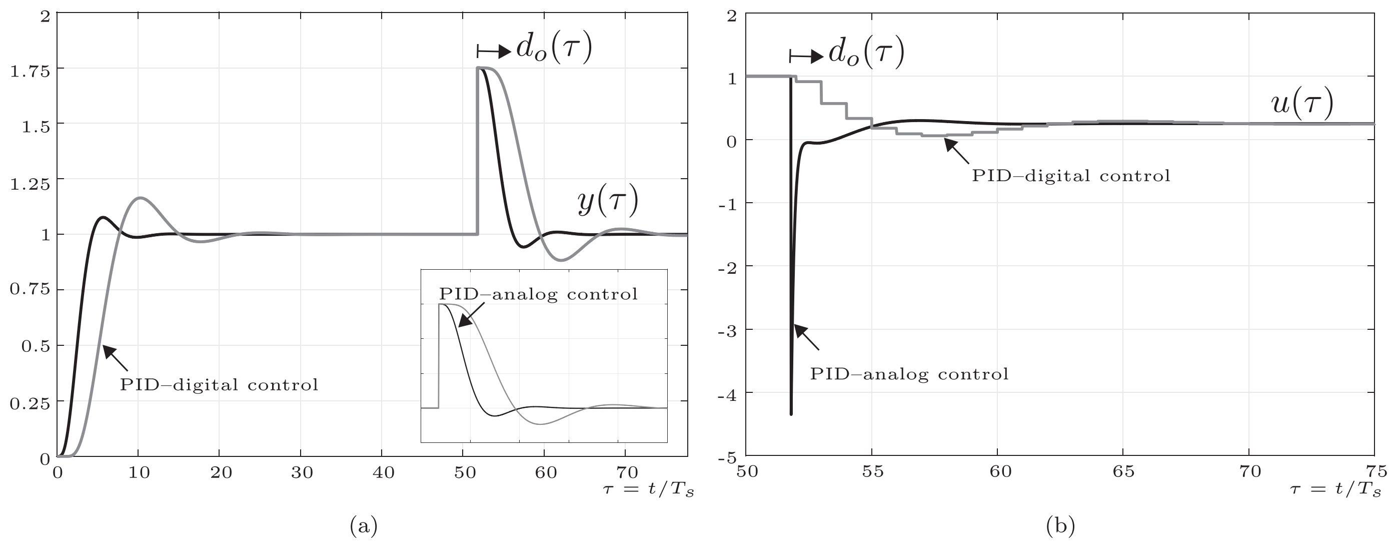

Fig. 14. Process G_p is defined by (74), analog controller is defined by (75) and digital controller is defined by (76) (a) Output $y(\tau)$ of the control loop at the presence of output disturbances, $\frac{T_{p1}}{T_s} = 1.25$, $ovs_{an} = 7.6\%$, $ovs_{dig} = 16.3\%$. (b) Control action $u(\tau)$ at the presence of output disturbance, $\frac{T_{p1}}{T_s} = 1.25$.

$$T_{i_{an}} = 2k_p k_h(\underbrace{\sum_{i=1}^{n} T_{p_i} + T_d + T_x}_{\text{sum of poles of } F_{OL}} - \sum_{i=1}^{m} T_{z_i} - X), \tag{66}$$

$$T_{i_{dig}} = 2k_h k_p(\underbrace{\sum_{i=1}^{n} (T_{p_i}) + T_d + T_x}_{\text{sum of poles of } F_{OL}} - \sum_{i=1}^{m} (T_{z_i}) - X - \frac{1}{2}T_s). \tag{67}$$

and X, Y PID controller parameters remain with the initial values calculated from the explicit proposed solution. For the process defined by (58) the initial PID controller for $t_x = 0$ is equal to (60). However and since such a design leads to an unacceptable response, the controller becomes PID–Lag with $t_x = 28$, $t_x = 24$, $t_x = 16$, where $t_x = \frac{T_x}{T_s}$. Initially we start with a high value of t_x in order to stabilize the control loop and start reducing its value gradually by achieving the proper performance depending on our application. In Fig. 13(a) the step response of the control loop is presented for three different values of parameter t_x. The command signal $u(\tau)$ is also depicted in Fig. 13(b). The calculated PID–Lag controller is given by

$$C_{PID-dig}(s')\Big|_{t_x=28} = \left(\frac{1 + s'x + s'^2 y}{s' t_i (1 + s' t_{p_n})}\right)^* \frac{\left(1 - e^{-s'}\right)}{s'} \frac{1}{(1 + s' t_x)} \tag{68}$$

$$= \frac{1 + 60.47\, s' + 1276 s'^2}{24.36 s'^4 + 73.3 s'^3 + 147.5 s'^2 + 5.174\, s'} \tag{69}$$

$$C_{PID-dig}(s')\Big|_{t_x=24} = \left(\frac{1 + s'x + s'^2 y}{s' t_i (1 + s' t_{p_n})}\right)^* \frac{\left(1 - e^{-s'}\right)}{s'} \frac{1}{(1 + s' t_x)} \tag{70}$$

$$= \frac{1 + 60.47\, s' + 1276 s'^2}{18.6 s'^4 + 56 s'^3 + 112.8 s'^2 + 4.603\, s'} \tag{71}$$

$$C_{PID-dig}(s')\Big|_{t_x=16} = \left(\frac{1 + s'x + s'^2 y}{s' t_i (1 + s' t_{p_n})}\right)^* \frac{\left(1 - e^{-s'}\right)}{s'} \frac{1}{(1 + s' t_x)} \tag{72}$$

$$= \frac{1 + 60.47\, s' + 1276 s'^2}{9.37 s'^4 + 28.2 s'^3 + 57.1 s'^2 + 3.4\, s'} \tag{73}$$

for all three different values of the t_x time constant.

4. Sampling time effect investigation

In this section the effect of the sampling time T_s to the quality of the proposed PID control action, compared to the optimal analog design is investigated.

In the sequel, two curves are plotted within each figure. Given the transfer function of the plant $G(s)$, the response of the output $y(\tau)$ and the command signal $u(\tau)$ are investigated. To do this, both control loops are normalized with the sampling time T_s and the digital controller is implemented according to the relation $s' = sT_s$. In Sections 4.1, 4.2, 4.3, 4.4 the transfer function $G(s)$ is considered the same and different ratios of $\frac{T_{p1}}{T_s}$ are investigated.

4.1. Sampling time $\frac{T_{p1}}{T_s} = 1.25$

In this case the plant is given by

$$G(s') = \frac{1}{(1 + 1.25\, s')(1 + 0.97\, s')(1 + 0.84\, s')(1 + 0.42\, s')(1 + 0.37\, s')} \tag{74}$$

and analog and digital controllers are equal to

$$C_{PID-an}(s') = \frac{1 + 2.8\, s' + 2.11 s'^2}{0.29 s'^2 + 2.36\, s'} \tag{75}$$

and

$$C_{PID-dig}(s') = \frac{1 + 3.22\, s' + 2.99 s'^2}{5.28 s'^3 + 6.79 s'^2 + 4.52\, s'} \tag{76}$$

respectively. In Fig. 14(a), (b) the output $y(\tau)$ and command signal response $u(\tau)$ at the presence of output disturbance $d_o(\tau)$. Peak overshoot for digital control action is 16.3% whereas for analog control action is 7.6%. The corresponding settling t_{ss} time is

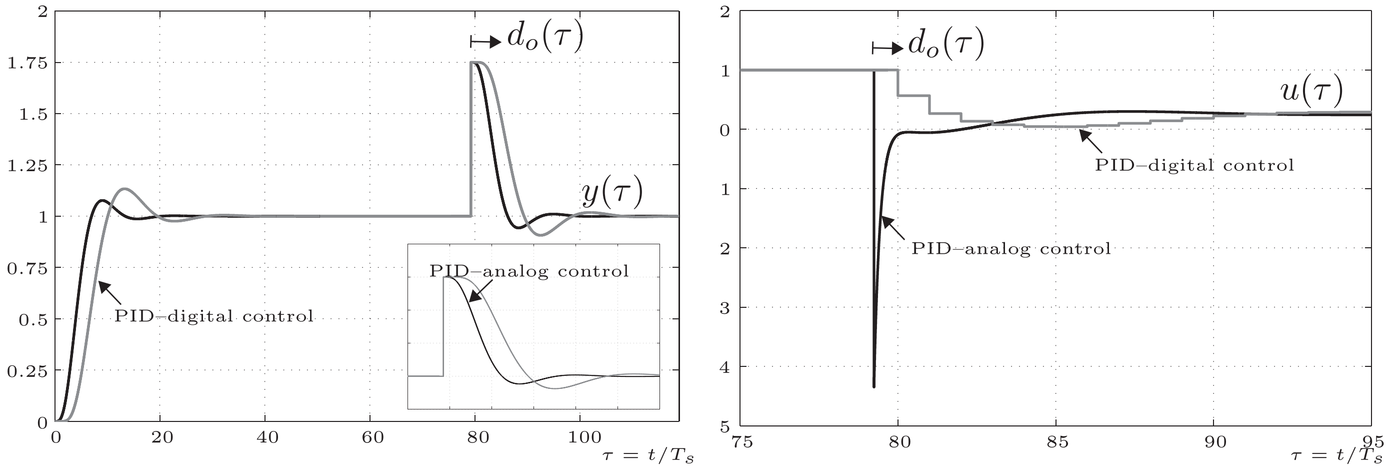

(a) (b)

Fig. 15. Process G_p is defined by (77), analog controller is defined by (78) and digital controller is defined by (79) (a) Output $y(\tau)$ of the control loop at the presence of output disturbances, $\frac{T_{p_1}}{T_s} = 2$, $ovs_{an} = 7.6\%$, $ovs_{dig} = 13.3\%$ (b) Control action $u(\tau)$ at the presence of output disturbance, $\frac{T_{p_1}}{T_s} = 2$.

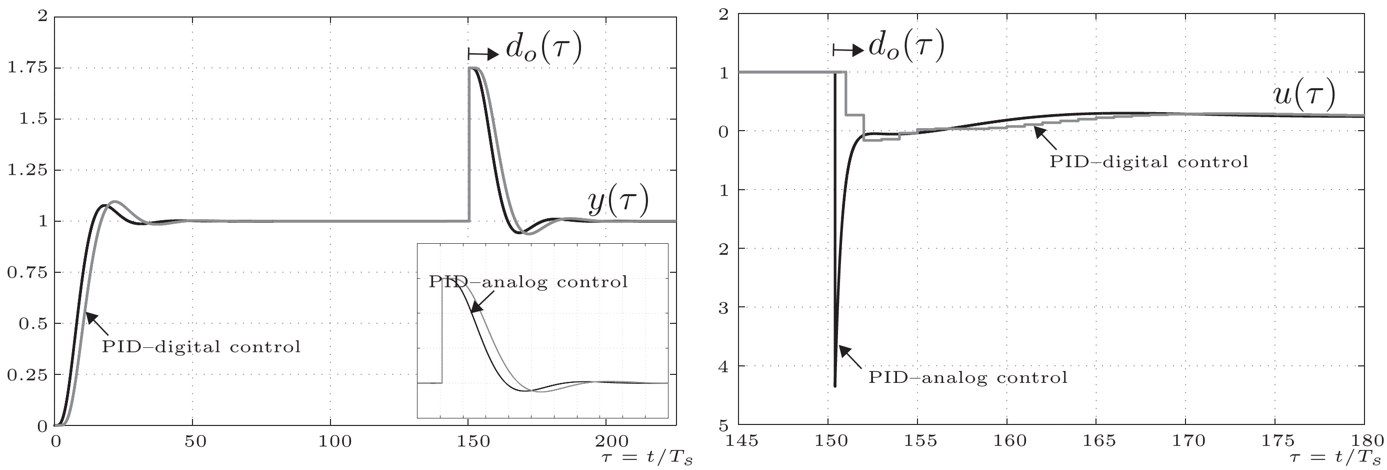

(a) (b)

Fig. 16. Process G_p is defined by (80), analog controller is defined by (81) and digital controller is defined by (82) (a) Output $y(\tau)$ of the control loop at the presence of output disturbances, $\frac{T_{p_1}}{T_s} = 4$, $ovs_{an} = 7.6\%$, $ovs_{dig} = 8.5\%$ (b) Control action $u(\tau)$ at the presence of output disturbance, $\frac{T_{p_1}}{T_s} = 4$.

$t_{ss} = 7.6\tau$ for analog and $t_{ss} = 21\tau$ digital control action respectively.

4.2. Sampling time $\frac{T_{p_1}}{T_s} = 2$

In this example the transfer function of the plant is defined by

$$G(s') = \frac{1}{(1 + 2\,s')(1 + 1.55\,s')(1 + 1.34\,s')(1 + 0.67\,s')(1 + 0.59\,s')} \tag{77}$$

whereas the analog and digital control actions are defined by

$$C_{PID-an}(s') = \frac{1 + 4.48\,s' + 5.4s'^2}{0.75s'^2 + 3.78\,s'} \tag{78}$$

$$C_{PID-dig}(s') = \frac{1 + 4.89\,s' + 6.66s'^2}{6.96s'^3 + 8.95s'^2 + 5.97\,s'} \tag{79}$$

respectively. After reducing controller's sampling time T_s, both step and command signal responses are improved compared to the previous example as observed in Fig. 15(a), (b) respectively. Peak overshoot for digital control action is 13.3% whereas for analog control action is 7.6%. The corresponding settling t_{ss} time is $t_{ss} = 7.6\tau$ and $t_{ss} = 17\tau$ for analog and digital control law respectively. Digital command signal response depicted in Figs. 14(b), 15(b) does not exhibit undesired peaks as observed in the analog control action.

4.3. Sampling time $\frac{T_{p_1}}{T_s} = 4$

In this example the transfer function of the plant is defined by

$$G(s') = \frac{1}{(1 + 4\,s')(1 + 3.11\,s')(1 + 2.69\,s')(1 + 1.35\,s')(1 + 1.18\,s')} \tag{80}$$

whereas calculated analog and digital control actions are given by

$$C_{PID-an}(s') = \frac{1 + 8.97\,s' + 21.6s'^2}{3.02s'^2 + 7.56\,s'} \tag{81}$$

and

$$C_{PID-dig}(s') = \frac{1 + 9.4\,s' + 24.25s'^2}{11.32s'^3 + 14.55s'^2 + 9.7\,s'} \tag{82}$$

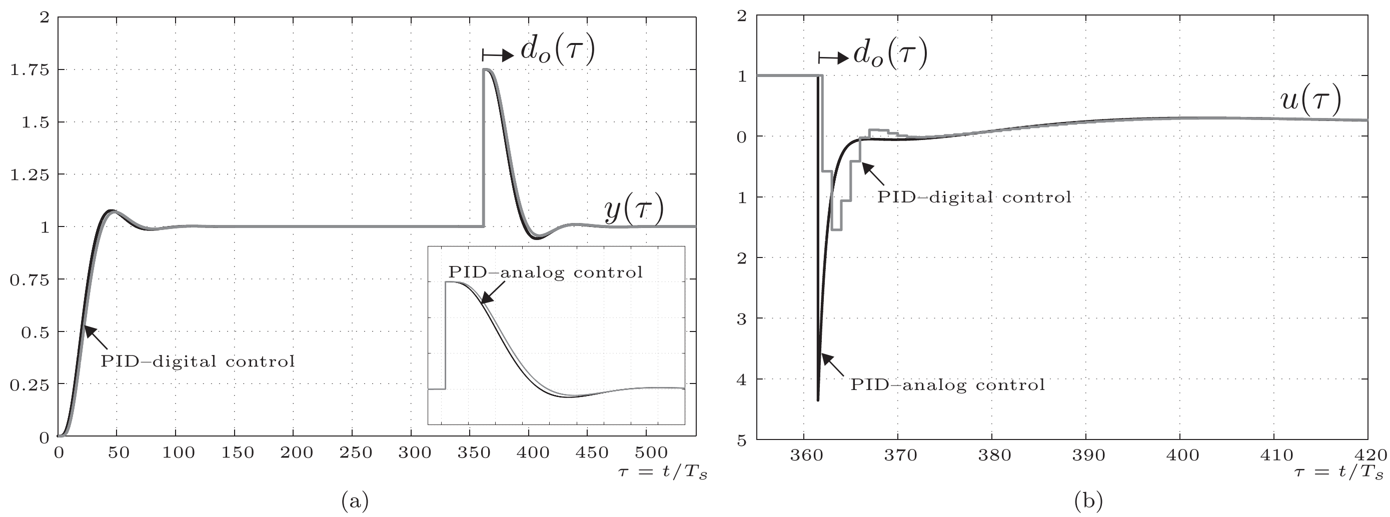

Fig. 17. Process G_p is defined by (83), analog controller is defined by (84) and digital controller is defined by (85) (a) Output $y(\tau)$ of the control loop at the presence of output disturbances, $\frac{T_{p1}}{T_s} = 10$, $ovs_{an} = 7.6\%$, $ovs_{dig} = 6.9\%$. (b) Control action $u(\tau)$ at the presence of output disturbance, $\frac{T_{p1}}{T_s} = 10$.

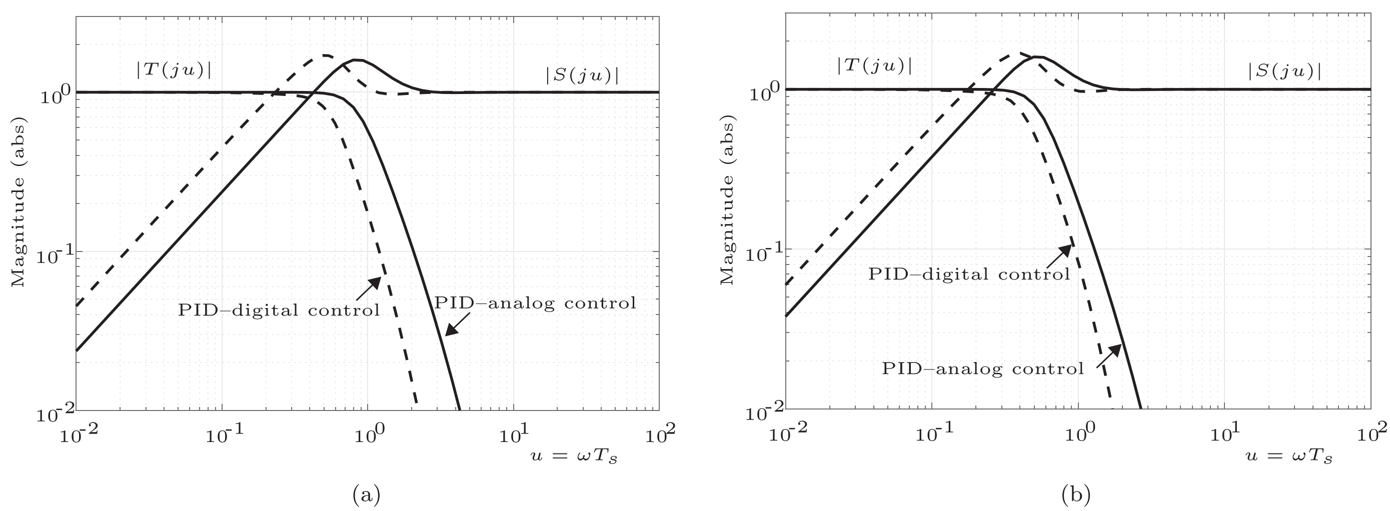

Fig. 18. Frequency response diagrams for analog and digital control loops as those presented in Sections 4.1 and 4.2 respectively (a) Frequency response of sensitivity $|S(ju)|$ and complementary sensitivity $|T(ju)|$ for $\frac{T_{p1}}{T_s} = 1.25$ (b) Frequency response of sensitivity $|S(ju)|$ and complementary sensitivity $|T(ju)|$ for $\frac{T_{p1}}{T_s} = 2$.

respectively. By further reducing sampling time T_s the trend of the responses of $y(\tau)$, $u(\tau)$ is similar to the ones observed in Section 4.2 respectively. Step response characteristics are further improved: overshoot value for digital control action is 8.5% and settling time is $t_{ss} = 34.3\tau$ for digital control compared to $t_{ss} = 24.4\tau$ regarding analog control action. Peak value for digital command signal response depicted in Fig. 16(b) has been slightly increased.

4.4. Sampling time $\frac{T_{p1}}{T_s} = 10$

In this example the transfer function of the plant is defined by

$$G(s') = \frac{1}{(1 + 10\,s')(1 + 7.79\,s')(1 + 6.73\,s')(1 + 3.39\,s')(1 + 2.97\,s')} \quad (83)$$

and the calculated analog and digital controllers are given by

$$C_{PID-an}(s') = \frac{1 + 22.43\,s' + 135.1s'^2}{18.9s'^2 + 18.91\,s'} \quad (84)$$

and

$$C_{PID-dig}(s') = \frac{1 + 22.96\,s' + 143.6s'^2}{24.32s'^3 + 31.26s'^2 + 20.8\,s'} \quad (85)$$

respectively. In this case both responses of $y(\tau)$ are almost identical as observed in Fig. 17(a). However, further sampling time reduction compared to previous examples has led to an increase in the command signal's peak value as observed in Fig. 17(b) regarding the digital control action.

In Figs. 18, 19 the frequency response diagrams for sensitivity S and complementary sensitivity T are presented, [27]. From there it is apparent that reduction of sampling time T_s shortens the region for which $|T(ju)| \simeq 1$. This behaviour is against the target of the Magnitude Optimum criterion, for which $|T(ju)| \simeq 1$ is desired in the widest possible frequency range. Therefore, sampling time T_s must be chosen such, so that step response $y(\tau)$ approaches the analog control loop response in such a manner which does not lead to high peak values of the command signal. Frequency response of the final control loop must also be observed, since shortening of the region for which $|T(ju)| \simeq 1$ makes the control loop more sensitive to possible disturbances in the low and high frequency region.

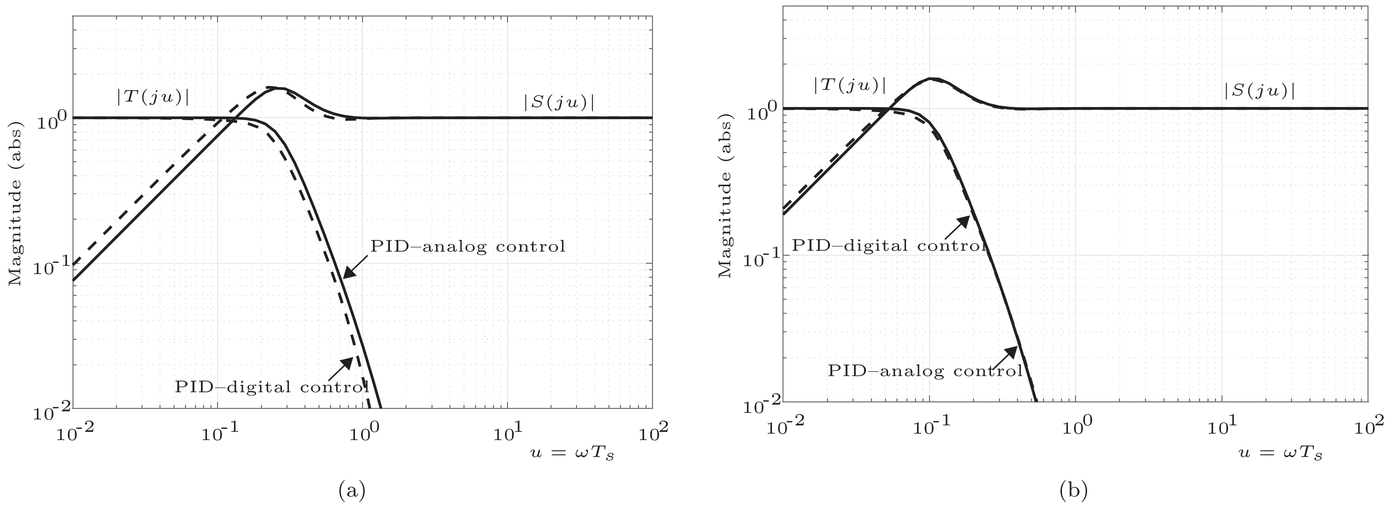

Fig. 19. Frequency response diagrams for analog and digital control loops as those presented in Sections 4.3 and 4.4 respectively (a) Frequency response of sensitivity $|S(ju)|$ and complementary sensitivity $|T(ju)|$ for $\frac{T_{p1}}{T_s} = 4$ (b) Frequency response of sensitivity $|S(ju)|$ and complementary sensitivity $|T(ju)|$ for $\frac{T_{p1}}{T_s} = 10$.

5. Conclusions

An explicit solution regarding the tuning of digital PID type controllers has been presented. The proposed control law can be applied in any linear stable SISO process regardless of its complexity. The proposed solution allows for 1) accurate examination of the effect of the controller's sampling time to the control loop's performance 2) decide when the control has to be I, PI or PID 3) optimal disturbance rejection at the output of the controlled process as it is frequently desired in many industry applications. To this end, control engineers would be capable of making accurate simulation of an industrial model, before integrating the PID controller within the software of a real time application. Examination of the effect of the controller's sampling time T_s to the control loop's performance revealed interesting trade–off features observed in the time and frequency domain responses. Future work will concentrate on 1) proposing solutions for handling the detrimental effects on the command signal that may appear because of the choice of sampling time 2) the definition of explicit PID digital control action for type–II, type–III[7] control loops along with experimental evaluation on a specific industrial application 3) examine how different transformations from the s to z domain affect the control loop's performance.

Acknowledgements

The authors would like to thank the two anonymous reviewers for their valuable feedback during the peer–review process.

Appendix A. Optimization conditions

In this section the optimization conditions that the proposed PID tuning method uses as a principle for developing the optimal control law are presented. Let the closed loop transfer function be defined by

$$T(s) = \frac{s^m b_m + s^{m-1} b_{m-1} + \cdots + s^2 b_2 + s b_1 + b_0}{s^n a_n + s^{n-1} a_{n-1} + \cdots + s^2 a_2 + s a_1 + a_0} = \frac{N(s)}{D(s)} \tag{A.1}$$

where $m \le n$. The target of the (MO) design criterion is to maintain $|T(s)| \simeq 1$ in the widest possible frequency range. Substituting $s = j\omega$ into (A.1) and squaring $|T(j\omega)|$ results in $T(j\omega)|^2 = \frac{|N(j\omega)|^2}{|D(j\omega)|^2}$ where

$$T(j\omega) = \frac{N(j\omega)}{D(j\omega)} = \frac{(j\omega)^m b_m + \cdots + (j\omega)^2 b_2 + (j\omega) b_1 + b_0}{(j\omega)^n a_n + \cdots + (j\omega)^2 a_2 + (j\omega) a_1 + a_0}. \tag{A.2}$$

Polynomials $N(j\omega)$ and $D(j\omega)$ are rewritten as follows

$$N(j\omega) \simeq \ldots + b_8\omega^8 - b_6\omega^6 + b_4\omega^4 - b_2\omega^2 + b_0 + j\left(\cdots - b_7\omega^7 + b_5\omega^5 - b_3\omega^3 + b_1\omega\right) \tag{A.3}$$

and

$$D(j\omega) \simeq \ldots + a_8\omega^8 - a_6\omega^6 + a_4\omega^4 - a_2\omega^2 + a_0 + j\left(\cdots - a_7\omega^7 + a_5\omega^5 - a_3\omega^3 + a_1\omega\right) \tag{A.4}$$

or

[7] Control loops with two and three integrators in the open loop transfer function, see [27]

$$
\begin{aligned}
|D(j\omega)|^2 \simeq\ & (a_8^2)\omega^{16} + (a_7^2 - a_8a_6)\omega^{14} + (a_6^2 + 2a_4a_8 - 2a_5a_7)\omega^{12} \\
& + (a_5^2 + 2a_3a_7 - 2a_2a_8 - 2a_4a_6)\omega^{10} \\
& + (a_4^2 + 2a_0a_8 + 2a_2a_6 - 2a_1a_7 - 2a_3a_5)\omega^{8} \\
& + (a_3^2 + 2a_1a_5 - 2a_6a_0 - 2a_2a_4)\omega^{6} + (a_2^2 + 2a_0a_4 - 2a_1a_3)\omega^{4} \\
& + (a_1^2 - 2a_0a_2)\omega^{2} + a_0\omega^0
\end{aligned}
\tag{A.5}
$$

and

$$
\begin{aligned}
|N(j\omega)|^2 \simeq\ & b_8^2\omega^{16} + (b_7^2 - b_8b_6)\omega^{14} + (b_6^2 + 2b_4b_8 - 2b_5b_7)\omega^{12} \\
& + (b_5^2 + 2b_3b_7 - 2b_2b_8 - 2b_4b_6)\omega^{10} \\
& \times (b_4^2 + 2b_0b_8 + 2b_2b_6 - 2b_1b_7 - 2b_3b_5)\omega^{8} \\
& + (b_3^2 + 2b_1b_5 - 2b_6b_0 - 2b_2b_4)\omega^{6} + (b_2^2 + 2b_0b_4 - 2b_1b_3)\omega^{4} \\
& + (b_1^2 - 2b_0b_2)\omega^{2} + (b_0)\omega^0.
\end{aligned}
\tag{A.6}
$$

By making equal the terms of ω^j, ($j = 1, 2, \ldots, n$) in polynomials $|D(j\omega)|^2$, $|N(j\omega)|^2$ results in

$$a_0 = b_0 \tag{A.7}$$

$$a_1^2 - 2a_2a_0 = b_1^2 - 2b_2b_0 \tag{A.8}$$

$$a_2^2 - 2a_3a_1 + 2a_4a_0 = b_2^2 - 2b_3b_1 + 2b_4b_0 \tag{A.9}$$

$$a_3^2 + 2a_1a_5 - 2a_6a_0 - 2a_4a_2 = b_3^2 + 2b_1b_5 - 2b_6b_0 - 2b_4b_2 \tag{A.10}$$

$$
\begin{aligned}
(a_4^2 + 2a_0a_8 + 2a_6a_2 - 2a_1a_7 - 2a_3a_5) &= (b_4^2 + 2b_0b_8 + 2b_6b_2 - 2b_1b_7 - 2b_3b_5) \\
\cdots &= \cdots
\end{aligned}
\tag{A.11}
$$

Further optimization conditions are not presented on purpose, because the current analysis sticks to the PID control law. However, if higher order controllers are designed, then further optimization conditions would essentially be required.

Appendix B. The revised digital PID control law

Given the process defined by

$$G(s) = \frac{s^m\beta_m + s^{m-1}\beta_{m-1} + \cdots + s^2\beta_2 + s\beta_1 + 1}{s^{n-1}\alpha_{n-1} + \cdots + s^3\alpha_3 + s^2\alpha_2 + s\alpha_1 + 1}e^{-sT_d} \tag{B.1}$$

the PID type controller

$$C(s) = C^*(s)C_{ZOH}(s) = \left(\frac{1 + sX + s^2Y}{sT_i(1 + sT_{p_n})}\right)^*\left(\frac{1 - e^{-sT_s}}{sT_s}\right) \tag{B.2}$$

is considered. $C^*(s)$ controller stands for the digital representation of the analog PID control action and $C_{ZOH}(s)$ stands for the zero order hold unit with sampling period T_s. For the needs of the mathematical analysis, the product is rewritten in the form of

$$
\begin{aligned}
C(s)G(s) = & \frac{s^m\beta_m + s^{m-1}\beta_{m-1} + \cdots + s^2\beta_2 + s\beta_1 + 1}{(s^{n-1}\alpha_{n-1} + \cdots + s^3\alpha_3 + s^2\alpha_2 + s\alpha_1 + 1)(1 + sT_{p_n})}e^{-sT_d} \\
& \left(\frac{1 + sX + s^2Y}{sT_i}\right)^*\left(\frac{1 - e^{-sT_s}}{sT_s}\right)
\end{aligned}
\tag{B.3}
$$

which is equal to

$$
\begin{aligned}
C(s)G(s) = & \frac{s^m\beta_m + s^{m-1}\beta_{m-1} + \cdots + s^2\beta_2 + s\beta_1 + 1}{(s^np_n + \cdots + s^3p_3 + s^2p_2 + sp_1 + 1)}e^{-sT_d} \\
& \left(\frac{1 + sX + s^2Y}{sT_i}\right)^*\left(\frac{1 - e^{-sT_s}}{sT_s}\right)
\end{aligned}
\tag{B.4}
$$

where

$$\begin{aligned}&(s^{n-1}\alpha_{n-1}+\cdots+s^3\alpha_3+s^2\alpha_2+s\alpha_1+1)(1+sT_{p_n})=\\&s^nT_{p_n}\alpha_{n-1}+s^{n-1}(T_{p_n}\alpha_{n-2}+\alpha_{n-1})+\cdots+s^3(\alpha_3+T_{p_n}\alpha_2)+\\&s^2(\alpha_2+T_{p_n}\alpha_1)+s(\alpha_1+T_{p_n})+1=\\&s^np_n+\cdots+s^3p_3+s^2p_2+sp_1+1.\end{aligned} \tag{B.5}$$

After normalizing all time constants in the frequency domain with the sampling period T_s and substituting

$$s'=sT_s \tag{B.6}$$

the resulting expressions for (B.2) and (1) are

$$G(s')=k_p\frac{s'^mz_m+\cdots+s'^4z_4+s'^3z_3+s'^2z_2+s'z_1+1}{s'^nr_n+s'^{n-1}r_{n-1}+\cdots+s'^5r_5+s'^4r_4+s'^3r_3+s'^2r_2+s'r_1+1}e^{-s'd} \tag{B.7}$$

and

$$C(s')=C^*(s')C_{ZOH}(s')=\left(\frac{1+s'x+s'^2y}{s't_i}\right)^*\left(\frac{1-e^{-s'}}{s'}\right) \tag{B.8}$$

respectively, where

$$x=\frac{X}{T_s},\ y=\frac{Y}{T_s^2},\ t_i=\frac{T_i}{T_s},\ d=\frac{T_d}{T_s}, \tag{B.9}$$

$$r_j=\frac{p_j}{T_s^j},\quad \forall\ j=1,\ldots n,\quad z_i=\frac{\beta_i}{T_s^i},\quad \forall\ i=1,\ldots m. \tag{B.10}$$

have been set. The transition from the Laplace domain to the z domain is accomplished by making the transformation

$$s'=\frac{z-1}{z} \tag{B.11}$$

and since $z=e^{s'}$ then

$$s'=\frac{e^{s'}-1}{e^{s'}}. \tag{B.12}$$

Therefore, the digital PID type controller at (B.8) takes the form

$$\begin{aligned}C(s')=&\ C^*(s')C_{ZOH}(s')\\=&\ \frac{1}{t_i}\frac{(1+x+y)e^{2s'}-(x+2y)e^{s'}+y}{e^{s'}(e^{s'}-1)}.\end{aligned} \tag{B.13}$$

By setting

$$\hat{x}=x+2y\quad\text{and}\quad\hat{y}=1+x+y \tag{B.14}$$

results in

$$x=2\hat{y}-\hat{x}-2\quad\text{and}\quad y=\hat{x}-\hat{y}+1. \tag{B.15}$$

By substituting Eqs. (B.15) into (B.13) results in

$$C(s')=C^*(s')C_{ZOH}(s')=\frac{1}{t_i}\frac{(1-e^{s'})\hat{x}+(e^{2s'}-1)\hat{y}+1}{e^{s'}(e^{s'}-1)}. \tag{B.16}$$

In addition, the respective open and closed loop transfer functions become

$$F_{ol}(s')=k_hC(s')G(s') \tag{B.17}$$

or

$$F_{ol}(s')=k_h\frac{k_p}{t_i}\frac{(s'^mz_m+\cdots+s'^3z_3+s'^2z_2+s'z_1+1)[(1-e^{s'})\hat{x}+(e^{2s'}-1)\hat{y}+1]}{(s'^nr_n+\cdots+s'^3r_3+s'^2r_2+s'r_1+1)e^{s'(d+1)}(e^{s'}-1)} \tag{B.18}$$

and

$$T(s')=\frac{C(s')G(s')}{1+k_hC(s')G(s')}=\frac{N(s')}{D(s')}=\frac{N(s')}{D_1(s')+k_hN(s')} \tag{B.19}$$

or

$$T(s') = \frac{k_p(s'^m z_m + \cdots + s'^3 z_3 + s'^2 z_2 + s' z_1 + 1)\left[(1-e^{s'})\hat{x} + (e^{2s'}-1)\hat{y} + 1\right]}{\left[\begin{array}{c} t_i(s'^n r_n + \cdots + s'^3 r_3 + s'^2 r_2 + s' r_1 + 1)e^{s'(d+1)}(e^{s'}-1) + \\ k_h k_p(s'^m z_m + \cdots + s'^3 z_3 + s'^2 z_2 + s' z_1 + 1)\left[(1-e^{s'})\hat{x} + (e^{2s'}-1)\hat{y} + 1\right] \end{array}\right]}. \tag{B.20}$$

Approximating the time delay constant by the Taylor series

$$e'^s = 1 + s' + \frac{1}{2!}s'^2 + \frac{1}{3!}s'^3 + \frac{1}{4!}s'^4 + \frac{1}{5!}s'^5 + \frac{1}{6!}s'^6 + \cdots \tag{B.21}$$

results in

$$e^{s'(1+d)} = 1 + d's' + \frac{1}{2!}d'^2 s'^2 + \frac{1}{3!}d'^3 s'^3 + \frac{1}{4!}d'^4 s'^4 + \frac{1}{5!}d'^5 s'^5 + \frac{1}{6!}d'^6 s'^6 + \cdots \tag{B.22}$$

where

$$d' = 1 + d. \tag{B.23}$$

Additionally,

$$e^{s'(1+d)}(e^{s'} - 1) = d_1 s' + d_2 s'^2 + d_3 s'^3 + d_4 s'^4 + d_5 s'^5 + d_6 s'^6 + d_7 s'^7 + \cdots \tag{B.24}$$

where

$$\begin{bmatrix} d_1 \\ d_2 \\ d_3 \\ d_4 \\ d_5 \\ \vdots \end{bmatrix} = \begin{bmatrix} 1 \\ \frac{1}{2!} + d' \\ \frac{1}{3!} + \frac{1}{2!}d' + \frac{1}{2!}d'^2 \\ \frac{1}{4!} + \frac{1}{3!}d' + \frac{1}{2!}\frac{1}{2!}d'^2 + \frac{1}{3!}d'^3 \\ \frac{1}{5!} + \frac{1}{4!}d' + \frac{1}{2!}\frac{1}{3!}d'^2 + \frac{1}{2!}\frac{1}{3!}d'^3 + \frac{1}{4!}d'^4 \\ \vdots \end{bmatrix} \tag{B.25}$$

and with the help of (10)

$$\begin{bmatrix} q_1 \\ q_2 \\ q_3 \\ q_4 \\ q_5 \\ \vdots \end{bmatrix} = \begin{bmatrix} 1 \\ r_1 + d_2 \\ r_2 + r_1 d_2 + d_3 \\ r_3 + r_2 d_2 + r_1 d_3 + d_4 \\ r_4 + r_3 d_2 + r_2 d_3 + r_1 d_4 + d_5 \\ \vdots \end{bmatrix}. \tag{B.26}$$

For that reason, polynomial $D_1(s')$ and along with the help of (B.26), can be rewritten in the form of

$$D_1(s') = t_i(\cdots + q_7 s'^7 + q_6 s'^6 + q_5 s'^5 + q_4 s'^4 + q_3 s'^3 + q_2 s'^2 + s') \tag{B.27}$$

Making use of (B.21)–(B.23), the numerator of $C(s')$ is then equal to

$$\begin{aligned}(1-e^{s'})\hat{x} + (e^{2s'}-1)\hat{y} + 1 = {} & 1 + (2\hat{y} - \hat{x})s' + \frac{1}{2!}(4\hat{y} - \hat{x})s'^2 \\ & + \frac{1}{3!}(8\hat{y} - \hat{x})s'^3 + \frac{1}{4!}(16\hat{y} - \hat{x})s'^4 \\ & + \frac{1}{5!}(32\hat{y} - \hat{x})s'^5 + \frac{1}{6!}(64\hat{y} - \hat{x})s'^6 + \cdots. \end{aligned} \tag{B.28}$$

After some calculus at the numerator of the closed loop transfer function it is obtained

$$N(s') = k_p\left[\begin{array}{l} \cdots + (z_6 + y_6\hat{y} - x_6\hat{x})s'^6 + \\ (z_5 + y_5\hat{y} - x_5\hat{x})s'^5 + (z_4 + y_4\hat{y} - x_4\hat{x})s'^4 + \\ (z_3 + y_3\hat{y} - x_3\hat{x})s'^3 + (z_2 + y_2\hat{y} - x_2\hat{x})s'^2 + (z_1 + 2\hat{y} - \hat{x})s' + 1 \end{array}\right] \tag{B.29}$$

where

$$\begin{bmatrix} x_2 \\ x_3 \\ x_4 \\ x_5 \\ x_6 \\ \vdots \end{bmatrix} = \begin{bmatrix} z_1 + \frac{1}{2!} \\ z_2 + \frac{1}{2!}z_1 + \frac{1}{3!} \\ z_3 + \frac{1}{2!}z_2 + \frac{1}{3!}z_1 + \frac{1}{4!} \\ z_4 + \frac{1}{2!}z_3 + \frac{1}{3!}z_2 + \frac{1}{4!}z_1 + \frac{1}{5!} \\ z_5 + \frac{1}{2!}z_4 + \frac{1}{3!}z_3 + \frac{1}{4!}z_2 + \frac{1}{5!}z_1 + \frac{1}{6!} \\ \vdots \end{bmatrix}. \tag{B.30}$$

and

$$\begin{bmatrix} y_2 \\ y_3 \\ y_4 \\ y_5 \\ y_6 \\ \vdots \end{bmatrix} = \begin{bmatrix} 2z_1 + \frac{4}{2!} \\ 2z_2 + \frac{4}{2!}z_1 + \frac{8}{3!} \\ 2z_3 + \frac{4}{2!}z_2 + \frac{8}{3!}z_1 + \frac{16}{4!} \\ 2z_4 + \frac{4}{2!}z_3 + \frac{8}{3!}z_2 + \frac{16}{4!}z_1 + \frac{32}{5!} \\ 2z_5 + \frac{4}{2!}z_4 + \frac{8}{3!}z_3 + \frac{16}{4!}z_2 + \frac{32}{5!}z_1 + \frac{64}{6!} \\ \vdots \end{bmatrix}. \tag{B.31}$$

Finally, the corresponding polynomials for both the numerator and denominator of the closed loop transfer function are given by

$$\begin{aligned} D(s') = \; & D_1(s') + k_h N(s') = \cdots + \left[t_i q_6 + k_h k_p (z_6 + y_6 \hat{y} - x_6 \hat{x}) \right] s'^6 + \left[t_i q_5 + k_h k_p (z_5 + y_5 \hat{y} - x_5 \hat{x}) \right] s'^5 \\ & + \left[t_i q_4 + k_h k_p (z_4 + y_4 \hat{y} - x_4 \hat{x}) \right] s'^4 + \left[t_i q_3 + k_h k_p (z_3 + y_3 \hat{y} - x_3 \hat{x}) \right] s'^3 \\ & + \left[t_i q_2 + k_h k_p (z_2 + y_2 \hat{y} - x_2 \hat{x}) \right] s'^2 + \left[t_i + k_h k_p (z_1 + 2\hat{y} - \hat{x}) \right] s' + k_h k_p \end{aligned} \tag{B.32}$$

and

$$\begin{aligned} N(s') = \; & \cdots + k_p (z_6 + y_6 \hat{y} - x_6 \hat{x}) s'^6 + k_p (z_5 + y_5 \hat{y} - x_5 \hat{x}) s'^5 + k_p (z_4 + y_4 \hat{y} - x_4 \hat{x}) s'^4 \\ & + k_p (z_3 + y_3 \hat{y} - x_3 \hat{x}) s'^3 + k_p (z_2 + y_2 \hat{y} - x_2 \hat{x}) s'^2 + k_p (z_1 + 2\hat{y} - \hat{x}) s' + k_p. \end{aligned} \tag{B.33}$$

For determining the optimal PID controller's parameters, equations (A.7)–(A.10) will be applied to (B.20). For that reason, from the application of

Optimization condition: $a_0 = b_0$,

to the closed loop transfer function (B.19) along with (B.32), (B.33) results in

$$k_h = 1. \tag{B.34}$$

which implies that the final closed loop control system exhibits zero steady position error if $k_h = 1$.

Optimization condition: $a_1^2 - 2a_2 a_0 = b_1^2 - 2b_2 b_0$.

The second optimization condition results in

$$t_i = 2k_h k_p (r_1 + d_2 + \hat{x} - 2\hat{y} - z_1), \tag{B.35}$$

or according to (B.14), (B.15)

$$t_i = 2k_h k_p (r_1 + d - z_1 - x - \frac{1}{2}). \tag{B.36}$$

Optimization condition: $a_2^2 - 2a_3 a_1 + 2a_4 a_0 = b_2^2 - 2b_3 b_1 + 2b_4 b_0$.

The application of the third optimization condition to the closed loop transfer function results in

$$\begin{aligned} & \left[(q_2^2 - q_3) - (q_2 x_2 - x_3) \right] \hat{x} - \left[2(q_2^2 - q_3) - (q_2 y_2 - y_3) \right] \hat{y} \\ = \; & (q_3 z_1 - q_2 z_2 + z_3 - q_4) - (q_2^2 - 2q_3)(q_2 - z_1). \end{aligned} \tag{B.37}$$

Optimization condition: $a_3^2 + 2a_1 a_5 - 2a_6 a_0 - 2a_4 a_2 = b_3^2 + 2b_1 b_5 - 2b_6 b_0 - 2b_4 b_2$.

Finally the application of the fourth optimization condition to the closed loop transfer function leads to

$$\Big[(q_3-x_3)q_3-(q_4-x_4)q_2-(q_2-x_2)q_4+q_5-x_5\Big]\hat{x}$$
$$-\Big[2q_3^2-4q_2q_4+q_2y_4-q_3y_3-y_5+2q_5+q_4y_2\Big]\hat{y}$$
$$=-(q_3^2-2q_2q_4+2q_5)(q_2-z_1)$$
$$+(q_2z_4-q_3z_3+q_4z_2-q_5z_1-z_5+q_6). \tag{B.38}$$

To that end, the optimal PID controller's parameters are given by

$$k_h=1. \tag{B.39}$$

$$t_i=2k_hk_p(r_1+d-z_1-x-\frac{1}{2}) \tag{B.40}$$

$$\hat{x}-a_1\hat{y}=b_1 \quad \text{and} \quad \hat{x}-a_2\hat{y}=b_2 \tag{B.41}$$

where

$$a_1=\frac{2(q_2^2-q_3)-(q_2y_2-y_3)}{(q_2^2-q_3)-(q_2x_2-x_3)} \tag{B.42}$$

$$b_1=\frac{(q_3z_1-q_2z_2+z_3-q_4)-(q_2^2-2q_3)(q_2-z_1)}{(q_2^2-q_3)-(q_2x_2-x_3)} \tag{B.43}$$

$$a_2=\frac{2q_3^2-4q_2q_4+q_2y_4-q_3y_3-y_5+2q_5+q_4y_2}{(q_3-x_3)q_3-(q_4-x_4)q_2-(q_2-x_2)q_4+q_5-x_5} \tag{B.44}$$

$$b_2=\frac{-(q_3^2-2q_2q_4+2q_5)(q_2-z_1)+(q_2z_4-q_3z_3+q_4z_2-q_5z_1-z_5+q_6)}{(q_3-x_3)q_3-(q_4-x_4)q_2-(q_2-x_2)q_4+(q_5-x_5)} \tag{B.45}$$

By solving (B.40), (B.41) parameters $\hat{x}$, $\hat{y}$ are determined by

$$\hat{x}=\frac{a_1b_2-a_2b_1}{a_1-a_2}, \quad \hat{y}=\frac{b_2-b_1}{a_1-a_2} \tag{B.46}$$

From the definition of the integrator's time constant (B.40) it is critical to point out that

$$\frac{T_i}{T_s}=2k_hk_p(r_1+d-z_1-x-\frac{1}{2}) \tag{B.47}$$

or according to (B.9), (B.10)

$$\begin{aligned} T_i &= 2k_hk_p(T_sr_1+T_sd-T_sz_1-T_sx-\frac{1}{2}T_s) \\ &= 2k_hk_p(p_1+T_d-\beta_1-T_sx-\frac{1}{2}T_s) \\ &= 2k_hk_p(\sum_{i=1}^{n}(T_{p_i})+T_d-\sum_{i=1}^{m}(T_{z_i})-X-\frac{1}{2}T_s) \end{aligned} \tag{B.48}$$

In other words as it was proved in (18), integrator's time constant is equal

$$T_{i_{dig}}=T_{i_{an}}-2k_hk_p\frac{1}{2}T_s, \tag{B.49}$$

where $T_{i_{dig}}$ and $T_{i_{an}}$ the optimal values for the integrator's time constant regarding the digital and analog design respectively.

Appendix C. Calculated controller parameters

In this section the calculated controller parameters for the examples discussed in Section 3 for the analog and digital implementation are presented. All plots can be easily reproduced in Matlab/Simulink. Specifically, Figs. 3(a), (b) can be easily reproduced if all transfer functions (G_p, G_c, ZOH, k_h) are defined as LTI blocks in Matlab/Simulink workspace. For Section 3.1, G_p is defined by (49), G_c is defined by (51), and $k_h=1$ as proved in (B.34). Since sampling time of the control loop is inherited[8], when inserting the ZOH block, its parameter should be set to 1.

C.1. Controller parameters for Section 3.1: $\frac{T_{p_1}}{T_s} = 20$

In this case the plant is defined by (49). The analog control action is given by

$$C_{PID-an}(s') = \frac{1 + s'x + s'^2 y}{s' t_i} \frac{1}{(1 + s' t_{p_n})} = \frac{1 + 44.85\, s' + 540.4 s'^2}{75.63 s'^2 + 37.82\, s'} \tag{C.1}$$

and the digital control action is given by

$$C_{PID-dig}(s') = \left(\frac{1 + s'x + s'^2 y}{s' t_i (1 + s' t_{p_n})} \right)^* \frac{(1 - e^{-s'})}{s'} = \frac{1 + 45.57\, s' + 564.5 s'^2}{45.95 s'^3 + 59.08 s'^2 + 39.39\, s'} \tag{C.2}$$

The step response and the command signal response of the closed loop control system and along with its response to input and output disturbances is presented in Figs. 4(a), (b).

C.2. Controller parameters for Section 3.1: $\frac{T_{p_1}}{T_s} = 100$

In this case the plant is defined by (49). The analog control action is given by

$$C_{PID-an}(s') = \frac{1 + s'x + s'^2 y}{s' t_i} \frac{1}{(1 + s' t_{p_n})} = \frac{1 + 224\, s' + 1351 s'^2}{1891 s'^2 + 189.1\, s'} \tag{C.3}$$

and the digital control action is given by

$$C_{PID-dig}(s') = \left(\frac{1 + s'x + s'^2 y}{s' t_i (1 + s' t_{p_n})} \right)^* \frac{(1 - e^{-s'})}{s'} = \frac{1 + 226.5\, s' + 1392 s'^2}{219 s'^3 + 281.5 s'^2 + 187.7\, s'} \tag{C.4}$$

The step reponse and the command signal response of the closed loop control system and along with its response to input and output disturbances is presented in Figs. 5(a), (b).

C.3. Controller parameters for Section 3.2: $\frac{T_{p_1}}{T_s} = 20$

In this case the plant is defined by (52). The analog control action is given by

$$C_{PID-an}(s') = \frac{1 + s'x + s'^2 y}{s' t_i} \frac{1}{(1 + s' t_{p_n})} = \frac{1 + 52.17\, s' + 930.2 s'^2}{194 s'^2 + 96.94\, s'} \tag{C.5}$$

and the digital control action is given by

$$C_{PID-dig}(s') = \left(\frac{1 + s'x + s'^2 y}{s' t_i (1 + s' t_{p_n})} \right)^* \frac{(1 - e^{-s'})}{s'} = \frac{1 + 58.57\, s' + 1124 s'^2}{99.05 s'^3 + 127.3 s'^2 + 84.9\, s'} \tag{C.6}$$

The step response and the command signal response of the closed loop control system and along with its response to input and output disturbances is presented in Figs. 7(a), (b).

C.4. Controller parameters for Section 3.2: $\frac{T_{p_1}}{T_s} = 100$

In this case the plant is defined by (52). The analog control action is given by

$$C_{PID-an}(s') = \frac{1 + s'x + s'^2 y}{s' t_i} \frac{1}{(1 + s' t_{p_n})} = \frac{1 + 260.9\, s' + 2325 s'^2}{4847 s'^2 + 484.7 s'} \tag{C.7}$$

and the digital control action is given by

$$C_{PID-dig}(s') = \left(\frac{1 + s'x + s'^2 y}{s' t_i (1 + s' t_{p_n})} \right)^* \frac{(1 - e^{-s'})}{s'} = \frac{1 + 292.5\, s' + 2812 s'^2}{479.1 s'^3 + 615.9 s'^2 + 410.6\, s'} \tag{C.8}$$

The step response and the command signal response of the closed loop control system and along with its response to input and output disturbances is presented in Figs. 8(a), (b).

C.5. Controller parameters for Section 3.3: $\frac{T_{p_1}}{T_s} = 20$

In this case the plant is defined by (55). The analog control action is given by

[8] T_s is the normalization time constant of the control loop

$$C_{PID-an}(s') = \frac{1 + s'x + s'^2 y}{s't_i}\frac{1}{(1 + s't_{p_n})} = \frac{1 + 54.79\,s' + 834s'^2}{181s'^2 + 90.49\,s'} \tag{C.9}$$

and the digital control action is given by

$$C_{PID-dig}(s') = \left(\frac{1 + s'x + s'^2 y}{s't_i(1 + s't_{p_n})}\right)^* \frac{(1 - e^{-s'})}{s'} = \frac{1 + 55.58\,s' + 867s'^2}{107.8s'^3 + 138.6s'^2 + 92.38\,s'} \tag{C.10}$$

The step response and the command signal response of the closed loop control system and along with its response to input and output disturbances is presented in Figs. 10(a), (b).

C.6. Controller parameters for Section 3.3: $\frac{T_{p_1}}{T_s} = 100$

In this case the plant is defined by (58). The analog control action is given by

$$C_{PID-an}(s') = \frac{1 + s'x + s'^2 y}{s't_i}\frac{1}{(1 + s't_{p_n})} = \frac{1 + 273.9\,s' + 2085s'^2}{4524s'^2 + 452.4\,s'} \tag{C.11}$$

and the digital control action is given by

$$C_{PID-dig}(s') = \left(\frac{1 + s'x + s'^2 y}{s't_i(1 + s't_{p_n})}\right)^* \frac{(1 - e^{-s'})}{s'} = \frac{1 + 276.2\,s' + 2137s'^2}{525.6s'^3 + 675.7s'^2 + 450.5\,s'} \tag{C.12}$$

The step reponse and the command signal response of the closed loop control system and along with its response to input and output disturbances is presented in Figs. 11(a), (b).

References

[1] Desbourough L, Miller R. Increasing customer value of industrial control performance monitoring, Honeywell's experience, In: Proceedings of the 6th International Conference on Chemical Process Control, vol. 98 of AIChE Symposium Series Number 326; 2002, pp. 169–189.
[2] Vlachos C, Williams D, Gomm JB. Solution to the Shell standard control problem using genetically tuned. Control Eng Pract 2002;10(2):151–63.
[3] Liu GP, Daley S, Optimal-tuning PID. control for industrial systems. Control Eng Pract 2001;9(1):1185–94.
[4] Wai RJ, Chuang LJD,KL. Design and implementation of a 2-DOF PID compensation for magnetic levitation systems. ISA Trans 2014;53(4):1216–22.
[5] Åstrom, H. T KJ. The future of PID control. Control Eng Pract 2001;9(11):1163–75.
[6] Khodabakhshian A, Edrisi M. A new robust PID load frequency controller. Control Eng Pract 2008;16(9):1069–80.
[7] Ang KH, Chong G, Li Y. PID control system analysis, design, and technology. IEEE Trans Control Syst Technol 2005;13(4):559–76.
[8] Åstrom KJ, HT. PID controllers: theory, design and tuning, 2nd Edition, Instrument Society of America; 1995.
[9] Rahimi AR, Syberg BM, Emadi A. Active damping in DC/DC power electronic converters: a novel method to overcome the problems of constant power loads. IEEE Trans Ind Electron 2009;56(5):1428–39.
[10] Dannehl J, Fuchs FW, Hansen S, Thogersen PB. Investigation of active damping approaches for PI-based current control of grid-connected pulse width modulation converters with LCL filters. IEEE Trans Ind Appl 2009;46(4):1509–17.
[11] Dannehl J, Liserre M, Fuchs FW. Filter-based active damping of voltage source converters with LCL Filter. IEEE Trans Ind Electron 2011;58(8):3623–33.
[12] Liu F, Wu B, Zargari N, Pande M. An active damping Method Using inductor-current feedback control for high-power PWM current-source rectifier. IEEE Trans Power Electron 2011;26(9):2580–7.
[13] Umland WJ, Safiuddin M. Magnitude and symmetric optimum criterion for the design of linear control systems: what is it and how does it compare with the others? IEEE Trans Ind Appl 1990;26(3):489–97.
[14] Papadopoulos KG. PID Controller Tuning: using the magnitude optimum criterion. Springer-Verlag; 2015.
[15] Mastorocostas C, Kioskeridis I, Margaris N. Thermal and slip effects on rotor time constant in vector controlled induction motor drives. IEEE Trans Power Electron 2006;21(2):495–504.
[16] Saeedifard M, Bakhshai A. Neuro-computing vector classification SVM schemes to integrate the overmodulation region in neutral point clamped (NPC) Converters. IEEE Trans Power Electron 2007;22(3):995–1004.
[17] Bakhshai AR, Joos G, Jain P, Hua J. Incorporating the overmodulation range in space vector pattern generators using a classification algorithm. IEEE Trans Power Electron 2000;15(1):83–94.
[18] Dong-Choon L, G-Myoung L. A novel overmodulation technique for space-vector PWM inverters. IEEE Trans Power Electron 1998;13(6):1144–51.
[19] Kerkman RJ, Leggate D, Seibel BJ, Rowan TM. Operation of PWM voltage source-inverters in the overmodulation region. IEEE Trans Ind Electron 1996;43(1):132–41.
[20] O'Dwyer A. Handbook of PI and PID controller tuning rules. 1st Edition. Imperial College Press; 2003.
[21] Oldenbourg RC, Sartorius H. A uniform approach to the optimum adjustment of control loops. Trans ASME 1954:1265–79.
[22] Papadopoulos KG, Papastefanaki EN, Margaris NI. Explicit analytical PID tuning rules for the design of type-III control loops. IEEE Trans Ind Electron 2013;60(10):4650–64.
[23] Papadopoulos KG, Margaris NI. Extending the Symmetrical Optimum criterion to the design of PID type-p control loops. J Process Control 2012;22(1):11–25.
[24] Cvejn J. The design of PID controller for non-oscillating time-delayed plants with guaranteed stability margin based on the modulus optimum criterion. J Process Control 2013;23(4):570–84.
[25] Vrančić D, Strmčnik S, Juričić D. A magnitude optimum multiple integration tuning method for filtered PID controller. Automatica 2001;37(9):1473–9.
[26] Vrančić D, Strmčnik S, Kocijan J, Moura Oliveira P. Improving disturbance rejection of PID controllers by means of the magnitude optimum method. ISA Trans 2010;49(1):47–56.
[27] Papadopoulos KG, Tselepis N, Margaris NI. Revisiting the Magnitude Optimum criterion for robust tuning of PID Type-I Control loops. J Process Control 2012;22(6):1063–78.
[28] Papafotiou G, Kley J, Papadopoulos KG, Bohren P, Morari M. Model predictive direct torque control-Part II: implementation and experimental evaluation. IEEE Trans Ind Electron 2009;56(6):1906–15.